General Disclaimer

One or more of the Following Statements may affect this Document

- This document has been reproduced from the best copy furnished by the organizational source. It is being released in the interest of making available as much information as possible.

- This document may contain data, which exceeds the sheet parameters. It was furnished in this condition by the organizational source and is the best copy available.

- This document may contain tone-on-tone or color graphs, charts and/or pictures, which have been reproduced in black and white.

- This document is paginated as submitted by the original source.

- Portions of this document are not fully legible due to the historical nature of some of the material. However, it is the best reproduction available from the original submission.

E83-10158
TM-85217

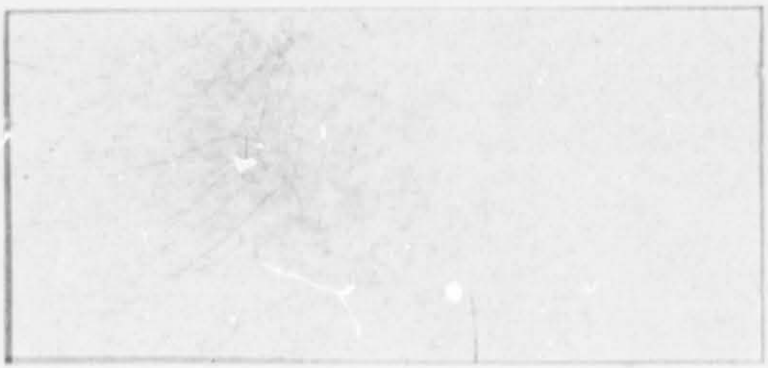

(E83-10158) OFF-NADIR ANTENNA BIAS CORRECTION USING AMAZON RAIN FOREST SIGMA NEG DATA (NASA) 69 p HC A04/MF A01 CSCL 02F

N83-17924

Unclas
G3/43 00158

THE UNIVERSITY OF KANSAS CENTER FOR RESEARCH, INC.
2291 Irving Hill Drive—Campus West
Lawrence, Kansas 66045

OFF-NADIR ANTENNA BIAS CORRECTION USING AMAZON RAIN FOREST σ^o DATA

by

I.J. Birrer*
E.M. Bracalente+
G.J. Dome°
J. Sweet+
G. Berthold*
R.K. Moore*

*University of Kansas Center for Research, Inc.
Lawrence, Kansas

+NASA Langley Research Center
Hampton, Virginia

°Bell Laboratories
Holmdel, New Jersey

Remote Sensing Laboratory
Center for Research, Inc.
The University of Kansas
Lawrence, Kansas 66045

RSL Technical Report
RSL TR 343-6

October 1981

Supported by:

NATIONAL AERONAUTICS AND SPACE ADMINISTRATION
NASA Langley Research Center
Hampton, Virginia 23665

CONTRACT NSG 1397

SECURITY CLASSIFICATION OF THIS PAGE (When Data Entered)

REPORT DOCUMENTATION PAGE		READ INSTRUCTIONS BEFORE COMPLETING FORM
1. REPORT NUMBER RSL TR 343-6	2. GOVT ACCESSION NO.	3. RECIPIENT'S CATALOG NUMBER
4. TITLE (and Subtitle) Off-Nadir Antenna Bias Correction Using Amazon Rain Forest σ° Data		5. TYPE OF REPORT & PERIOD COVERED 6. PERFORMING ORG. REPORT NUMBER RSL TR 343-6
7. AUTHOR(s) I.J. Birrer, E.M. Bracalente,° G.J. Dome,* J. Sweet,°G. Berthold, R.K. Moore °(NASA Langley) *Bell Laboratories		8. CONTRACT OR GRANT NUMBER(s) NSG 1397
9. PERFORMING ORGANIZATION NAME AND ADDRESS Remote Sensing Laboratory University of Kansas Center for Research, Inc. Lawrence, Kansas 66045		10. PROGRAM ELEMENT, PROJECT, TASK AREA & WORK UNIT NUMBERS
11. CONTROLLING OFFICE NAME AND ADDRESS NASA Langley Research Center Hampton, Virginia 23665		12. REPORT DATE October 1981 13. NUMBER OF PAGES 67
14. MONITORING AGENCY NAME & ADDRESS(if different from Controlling Office)		15. SECURITY CLASS. (of this report) Unclassified 15a. DECLASSIFICATION/DOWNGRADING SCHEDULE

16. DISTRIBUTION STATEMENT (of this Report)

Unlimited

17. DISTRIBUTION STATEMENT (of the abstract entered in Block 20, if different from Report)

18. SUPPLEMENTARY NOTES

19. KEY WORDS (Continue on reverse side if necessary and identify by block number)

20. ABSTRACT (Continue on reverse side if necessary and identify by block number)

The radar response from the Amazon rain forest has been studied to determine the suitability of this region for use as a standard target to calibrate a scatterometer like that proposed for the National Oceanic Satellite System (NOSS). Backscattering observations made by the SEASAT-1 Scatterometer System (SASS) show the Amazon rain forest to be a homogeneous, azimuthally-isotropic, radar target which is insensitive to polarization. The variation with angle of incidence may be adequately modeled as $\sigma^\circ_{(dB)} = a\theta + b$ with typical values

TABLE OF CONTENTS

LIST OF TABLES

LIST OF FIGURES

OFF-NADIR ANTENNA BIAS CORRECTION USING AMAZON RAIN FOREST σ^o DATA

I.J. Birrer*, E.M. Bracalente+, G.J. Dome°, J. Sweet+,
G. Berthold* and R.K. Moore*

ABSTRACT

The radar response from the Amazon rain forest has been studied to determine the suitability of this region for use as a standard target to calibrate a scatterometer like that proposed for the National Oceanic Satellite System (NOSS). Backscattering observations made by the SEASAT-1 Scatterometer System (SASS) show the Amazon rain forest to be a homogeneous, azimuthally-isotropic, radar target which is insensitive to polarization. The variation with angle of incidence may be adequately modeled as $\sigma^o_{(dB)} = a\theta + b$ with typical values for the incidence-angle coefficient from 0.07 - 0.15 dB/deg. A small diurnal effect occurs, with measurements at sunrise being 0.5 dB - 1 dB higher than the rest of the day.

Maximum-likelihood estimation algorithms presented here permit determination of relative bias and true pointing angle for each beam. Specific implementation of these algorithms for the proposed NOSS scatterometer system is also discussed.

*University of Kansas Center for Research, Inc., Lawrence, Kansas

+NASA Langley Research Center, Hampton, Virginia

°Bell Laboratories, Holmdel, New Jersey

1.0 INTRODUCTION

The National Oceanic Satellite System Scatterometer (NOSS SCATT) was designed to determine wind vectors on the ocean's surface by measuring radar backscatter from the surface. The SCATT was to be a fan-beam scatterometer utilizing six dual-polarized (V and H) antennas.

To achieve maximum wind-vector accuracy careful cross-calibration between antennas must be performed. This report discusses the development of a calibration technique utilizing measurements of the scattering coefficient σ^o from the Amazon rain forest. A brief discussion is presented of the method used to discriminate rain-forest signals from others. Maps (used to screen Brazil data) generated for this purpose are on a 0.25° x 0.25° grid for locating rivers and a 0.5° x 0.5° grid for identifying vegetation types.

The suitability of the Amazon rain forest for use as a calibration target is shown in Section 4.0. From July to October 1978 numerous backscatter measurements were made by the SEASAT-1 Scatterometer System (SASS). These measurements show the rain forest to be a homogeneous, azimuthally-isotropic radar target which is insensitive to polarization. Variation of σ^o with respect to incidence angle may be adequately modeled with a straight line fit of the form: $\sigma^o_{(dB)} = a\theta + b$, where θ is the angle of incidence (deg.). Measured values for the incidence angle coefficient, a, range from 0.07 - 0.15 dB/deg depending on beam and time of day. A small diurnal effect was observed with measurements made at sunrise (0500-0630) being consistently 0.5 - 1.0 dB higher than the rest of the day.

To cross-calibrate the beams on a multibeam scatterometer, two parameters, a relative bias and the true antenna pointing angle, must be determined for each beam. Development of two maximum-likelihood-estimation

algorithms to determine these parameters using Amazon rain forest data is discussed in Section 5.0. The first algorithm is used to determine both relative bias and true pointing angle. A second and considerably simpler version is then developed to monitor long-term changes in relative bias due to drift in the transmitter power. Specific processing required to implement these algorithms for the SCATT is also discussed in Section 5.0.

2.0 BACKGROUND

During the SEASAT program, the need for in-flight cross-calibration for antennas from a multibeam scatterometer became apparent. The originally proposed procedure using aircraft underflights proved inadequate. Based on the consistency of σ^0 data over the rain forest obtained during SKYLAB, R.K. Moore of The University of Kansas suggested using the Amazon rain forest data as a means of calibration.

The accompanying map (Figure 1) shows the vast extent of the Amazon rain forest. It includes an area of more than 3,000,000 km^2. Because of its equatorial location, seasonal effects are minimized and vegetation is always present. The region is very flat and uniformly forested except for breaks in the canopy over the Amazon River and its principal tributaries. The predominant climate is hot and humid, with annual precipitation as high as 3000 mm. A slight decrease in rainfall is observed in the large central part of the rain forest during the months of October to December. A similar decrease takes place in the northern part during the months of June to September. In the northwest a more significant decrease in rainfall occurs during May and June with the lowest rainfall in July and August.

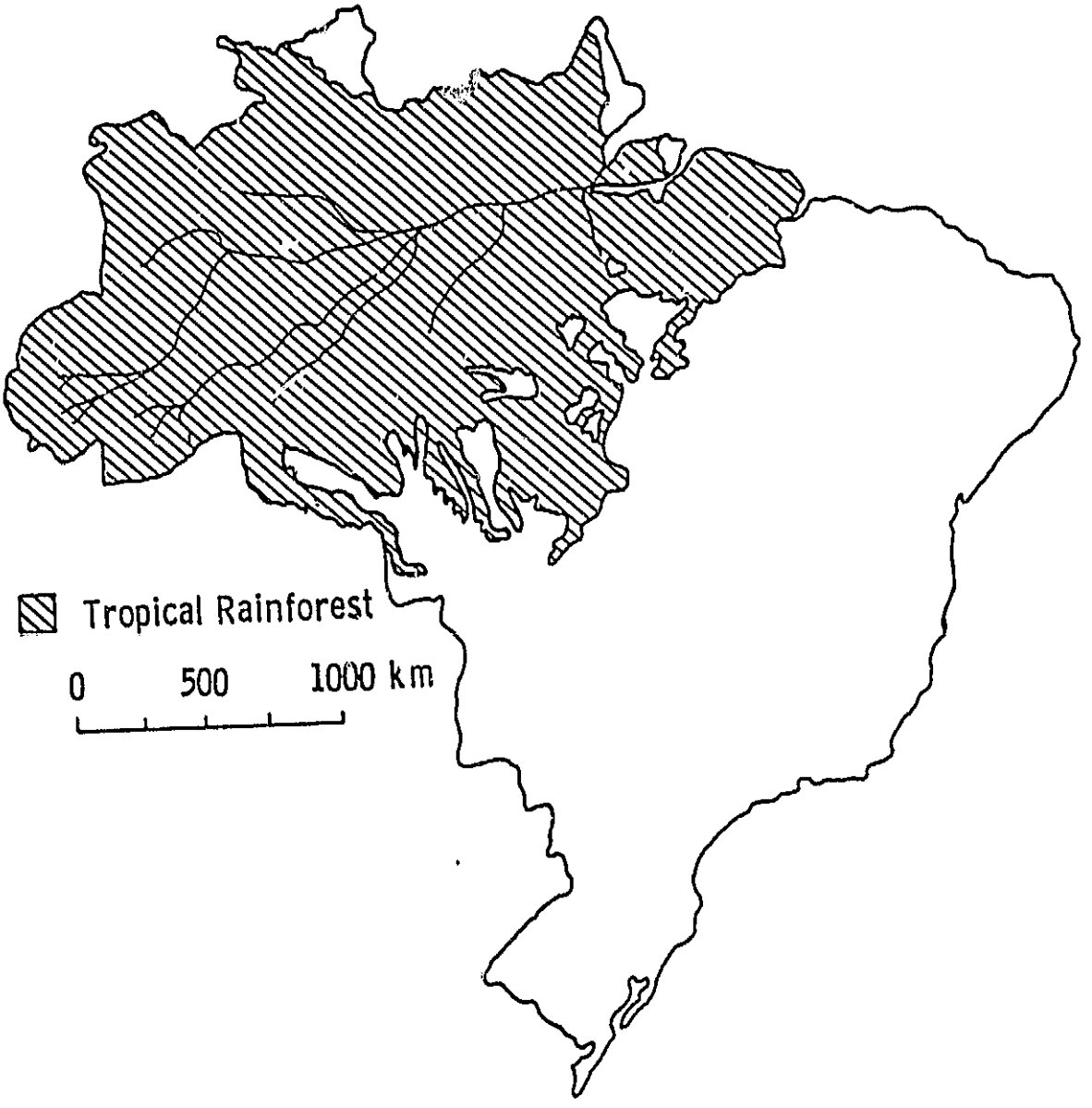

FIGURE 1: Extent of Brazilian Rain Forest

During the SKYLAB SL-2 mission vertical-polarization measurements were made over the Amazon rain forest at incidence angles of 32° to 36°. Figure 2 shows a sample time history taken during one of the SKYLAB passes over the eastern part of the forest. The scattering coefficient was stable with a maximum deviation of about 0.2 dB. For the combined set of SKYLAB measurements the mean value of σ^0 was reported as ≈ -5.9 dB with a standard deviation of 1 dB [1,2]. This observed consistency prompted the further investigation using the SEASAT scatterometer.

3.0 DEVELOPMENT OF MAPS USED TO CLASSIFY BRAZIL TARGETS

3.1 Land-Water Map

For the early analysis of SEASAT observations of Brazil, discrimination was achieved by using vegetation maps developed during the SKYLAB program [2]. The 1° x 1° grid available was thought to be adequate. However, as noted in Section 4.2, the presence in the SASS footprint of the Amazon River or one of its principal tributaries markedly lowered the radar cross-section. Since the SCATT was planned to operate with an even smaller footprint, a finer map grid was needed to screen out data contaminated by the presence of rivers.

For NOSS a digitized map was created with a 0.25° x 0.25° grid. The source map was produced by the Department of Cartography of the Brazilian Institute of Geography in 1971. This map of the entire Amazon basin is scaled at approximately 3 inches per degree. The digitized map was created by overlaying grids to subdivide the source map into 0.25° boxes. Codes were then assigned to each box using the following conventions:

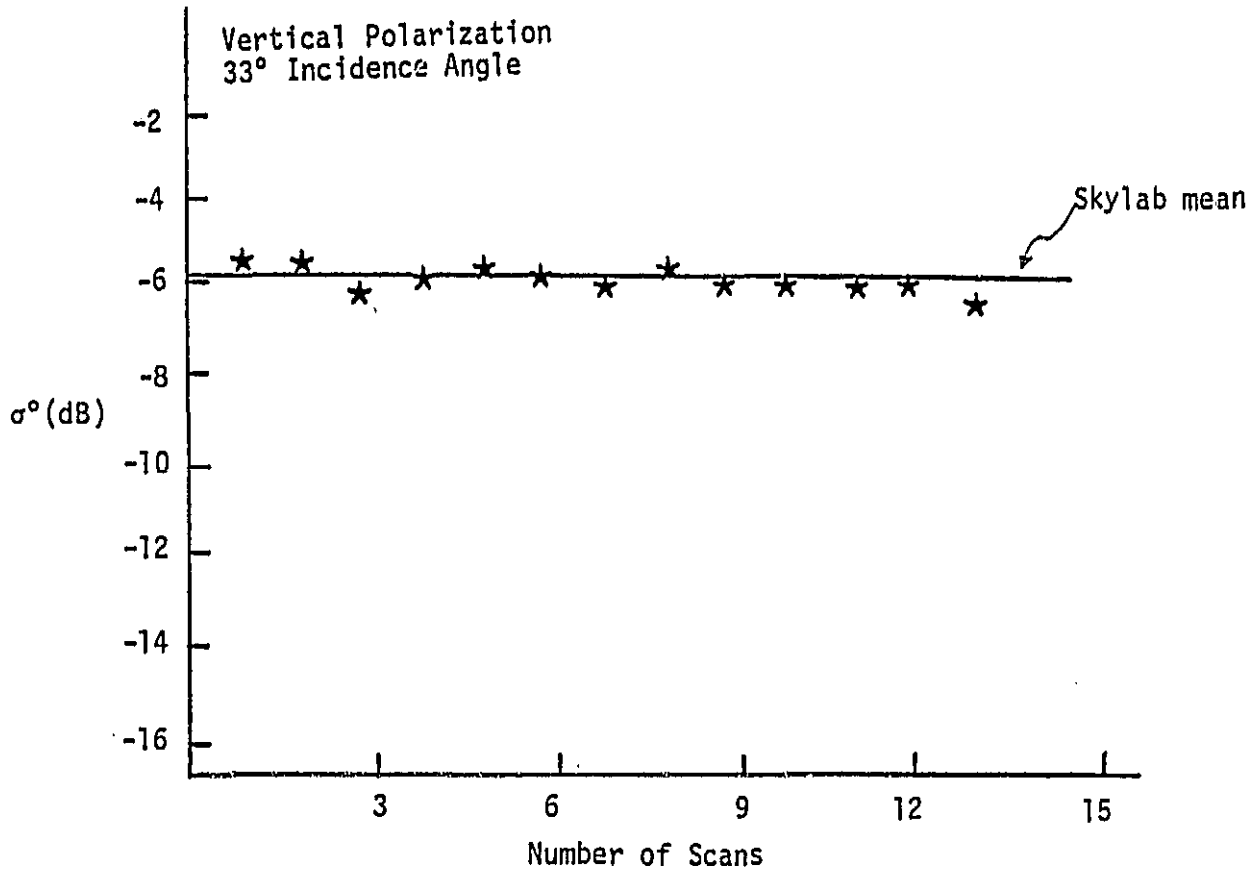

FIGURE 2: Sample SKYLAB Time History over Amazon Rain Forest

0 - flatland only (no significant rivers)

1 - some small rivers but mostly land

2 - large rivers through box

3 - rough terrain

The results of this procedure were then encoded into a computer algorithm. For a given latitude and longitude the algorithm will fetch the code of the box containing the location. This map was tested during the extensive analysis of SEASAT data discussed in Section 4.0.

For NOSS it was envisioned to use the computed location of the center of the Doppler cell for classification. A more careful screening could be performed by using the latitudes and longitudes of the corner points for a particular Doppler cell. Testing to be sure that all four corners showed a "land-only" condition would be a check against overlapping part of a river-filled box.

3.2 Vegetation Map

To further classify Brazilian data a vegetation map for the Amazon basin was produced with a 0.5° x 0.5° grid. Codes were assigned to each box according to the conventions listed in Table 1. Six distinct types of vegetation are found in the Amazon basin. Types 1 and 2 are the forests which are suitable for use as a standard target. Combinations of types were only designated if the dominant vegetation was either type 1 or type 2. Otherwise, they were coded with a 3, 4, 5, or 6, depending on the dominant type.

This map was incorporated into an algorithm similar to the land-water algorithm. For a particular latitude and longitude the code is retrieved for the box containing that location. This algorithm was used during the

TABLE 1
Codes Used in Vegetation Map

Type (Code)	Description
0	Outside of Brazil Rain Forest
1	Humid Upper Amazon
2	Humid Firm Land
3	Humid Floodlands
4	Humid Plains
5	Mountainous Region
6	Savannah
7	Combination Types 1,4
8	2,4
9	1,2,4
10	1,2
11	2,6
12	2,4,6
13	1,2,3,6
14	1,6
15	2,3,6
16	2,3
17	1,2,3
18	1,3
19	2,5
20	2,5,6

SASS analysis to remove all data from vegetation types 3,4,5, and 6. A similar approach is recommended for a NOSS-type of system.

4.0 CHARACTERIZATION OF σ^o SIGNATURE USING SEASAT SCATTEROMETER DATA

4.1 The SEASAT-A Scatterometer System (SASS)

The SASS operated using four dual-polarized (V and H) 0.5° x 25° fan-beam antennas. The antennas were pointed 45° from the satellite subtrack to give a "star-like" illumination pattern on the surface [3] (see Figure 3). This configuration provided for pairs of nearly orthogonal measurements of the earth's surface. The SASS instrument transmitted a 100-watt 14.6-GHz signal. The backscattered signal was spread out in frequency due to the Doppler effect. Using 15 parallel channels (each consisting of a Doppler filter, a square-law detector, and a gated integrator), the reflected power

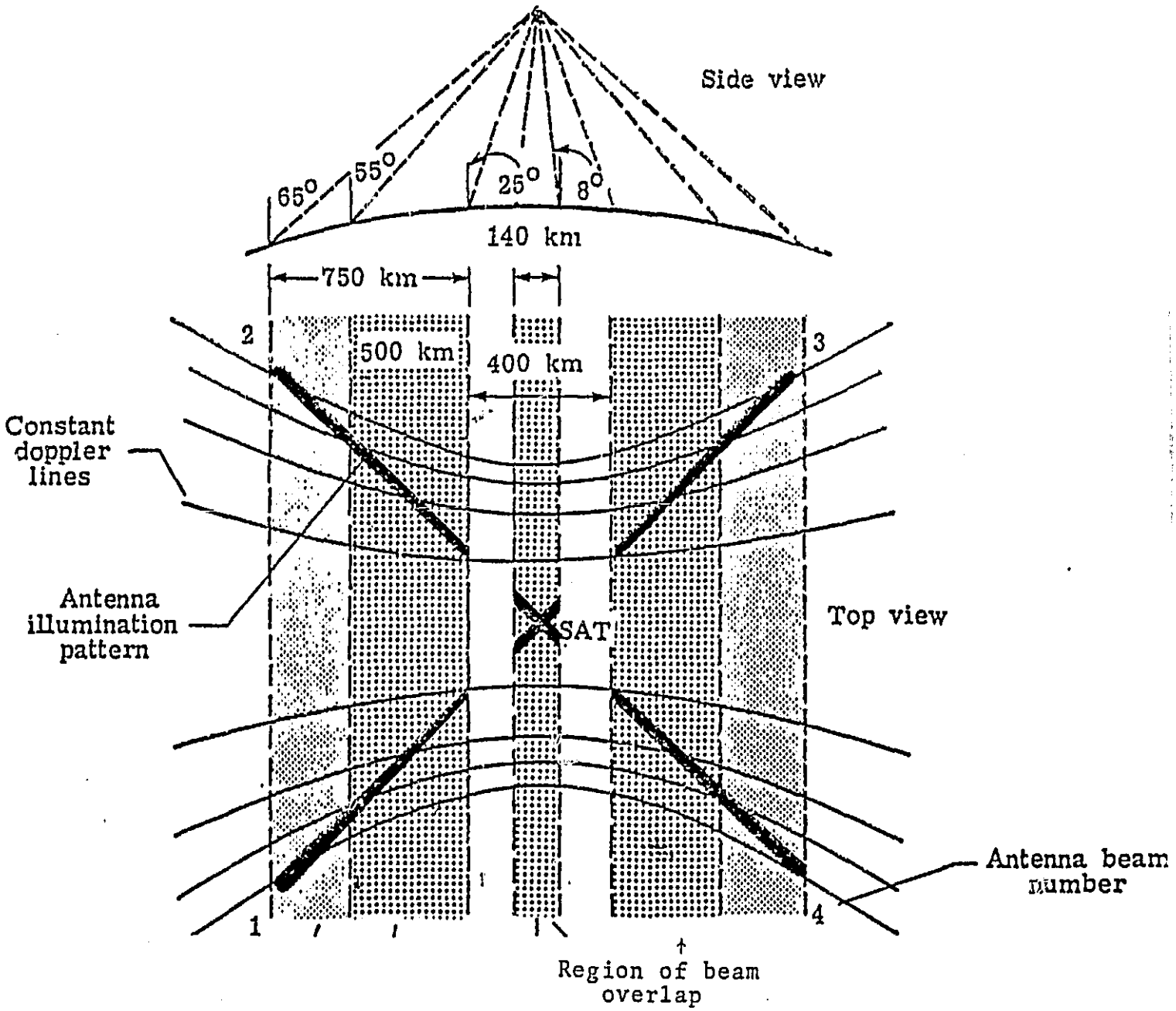

FIGURE 3: SEASAT Scatterometer Swath Coverage

from one antenna was sampled 61 times during a 1.89-sec measurement period. The mean values of the 61 integrated voltage levels of signal plus noise and noise alone from each of the 15 channels were transmitted to the ground. The power reflected from the earth's surface was determined from these voltage pairs, the calibrated gain of the receiver, and the known integration time, as indicated in Figure 4.

Figure 5 shows an enlarged view of one of the 15 Doppler cells synthesized along the beam. As illustrated, the Doppler-cell area is determined by the 0.5° 3-dB beamwidth in the narrow-beam plane and the Doppler filter along the beam. Due to the 1.89-sec measurement time the Doppler cell is smeared in the alongtrack direction to give the resultant cell shown in the lower inset. The integrated Doppler cells are between 16-20 km wide and 50-70 km long.

The frequencies selected for the Doppler filters result in three near-nadir resolution cells (0° - 13° incidence angle) and twelve off-nadir cells (20° - 65° incidence angle). Only the off-nadir measurements were used in this analysis since the near-nadir returns were outside the main antenna beam.

The value of σ^o can be determined by solving the radar equation in the following form:

$$P_R = \frac{P_T \lambda^2 L_S G_0^2}{(4\pi)^3} \int_A \frac{\left(\frac{G}{G_0}\right)^2 \sigma^o h(f)}{R^4} \, dA \qquad (1)$$

where:

P_R = received power

P_T = transmitted power

λ = transmitted wavelength

L_S = miscellaneous losses

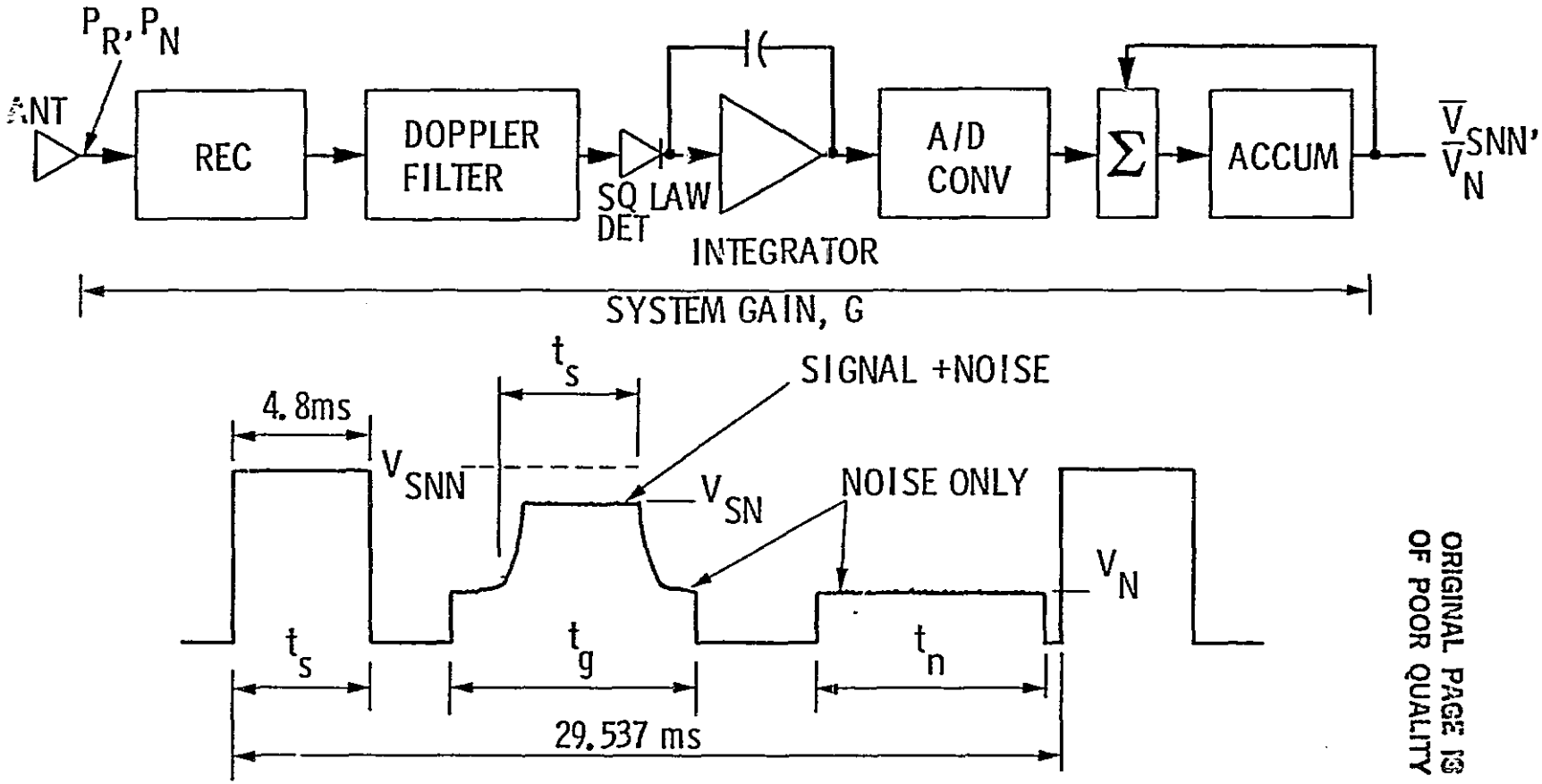

$T_S = 61 \times t_s = 0.2928$ (ALL CHANNELS)

$T_G = 61 \times t_g = 0.345$ TO 0.69

$T_N = 61 \times t_n = 0.4818$ (ALL CHANNELS)

$$V_{SNN} = T_S G (P_R + P_N) + (T_G - T_S) P_N G \quad (1)$$

$$\overline{V}_{SN} = \overline{V}_{SNN} - \frac{T_G - T_S}{T_N} \overline{V}_N \quad (2)$$

$$P_{SN} = \frac{\overline{V}_{SN}}{T_S G} \text{ - SIGNAL +NOISE POWER} \quad (3)$$

$$P_N = \frac{\overline{V}_N'}{T_N G} \text{ - NOISE POWER} \quad (4)$$

$$P_R = \frac{\overline{V}_{SN}}{T_S G} - \frac{\overline{V}_N}{T_N G} \text{ - SIGNAL POWER} \quad (5)$$

WHERE:

$$G = \frac{\overline{V}_{SNN} + \overline{V}_N}{P_N (T_G + T_N)} \quad (6)$$

FIGURE 4: Calculation of SASS Received Power

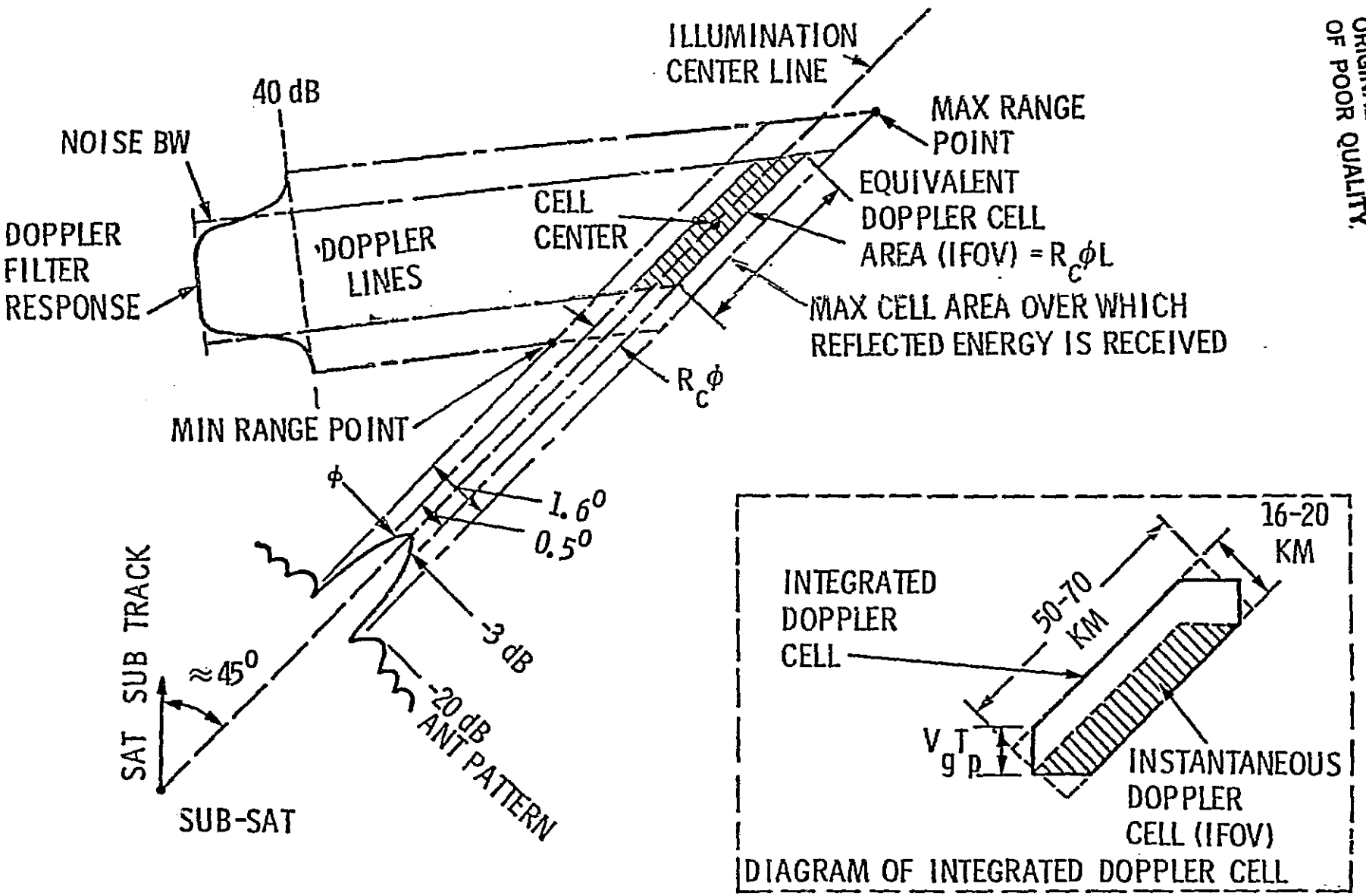

FIGURE 5: Doppler Cell Area Determined by Antenna Pattern and Filter Response

G_0 = peak antenna gain

$\frac{G}{G_0}$ = relative gain at center of cell

$h(f)$ = frequency response of Doppler filter

R = range to cell center

Equation (1) may be solved for σ^o as:

$$\sigma^o = \frac{(4\pi)^3 P_R R^4}{P_T \lambda^2 L_S G_0^2 (\frac{G}{G_0})^2 A} \tag{2}$$

assuming:

$$h(f) = \begin{cases} 1 & f_\ell < f < f_u \\ 0 & \text{otherwise} \end{cases}$$

where:

$A = L R\phi_A$, where L is the distance on earth's surface from f_ℓ to f_u

f_o = center frequency

B_n = noise bandwidth (Doppler filter)

f_ℓ, f_u = upper and lower Doppler-filter cutoff frequencies

ϕ_A = narrow dimension antenna beamwidth (radians)

$$f_\ell = f_o - \frac{B_n}{2}$$

$$f_u = f_o + \frac{B_n}{2}$$

A particular σ^o is calculated by evaluating equation (2) using measured values for P_R and P_T, values for G_0 and $\frac{G}{G_0}$ obtained from a lookup table, and computed values for R and A [4].

4.2 Target Stability of the Amazon Rain Forest

Initially the SASS data were processed by scientists at NASA Langley Research Center to produce time histories of σ^o over Brazil [4]. Figures

6 and 7 show sample time histories of Beam 1 vertical-polarization measurements made during an orbit identified as Rev 952. The radar-cross-section stability over the Amazon rain forest was similar to that observed during the SKYLAB mission. When the rain forest results are compared with the observations over the ocean, three striking differences are noted: (1) σ^o is consistently higher over the rain forest (except at the smallest incidence angle), (2) σ^o is much more stable over the rain forest, and (3) the variation in σ^o with incidence angle is much less. As can be seen in both Figures 6 and 7, SASS cells which included part of the Amazon or one of its major tributaries were easily identified by the sudden 1-3 dB drop in σ^o.

Since the goal of the research was to determine the Amazon rain forest's suitability as a standard target, tests were made for both temporal and regional stability. Comparing data taken at the same time of day over the same flight line throughout the mission provided a useful test for seasonal effects. Figure 8 shows the results of one of these comparisons. Approximately 5 measurements were averaged at each incidence angle to estimate the mean σ^o. The deviation of the mean σ^o is negligible near the peak antenna gain ($\theta_i = 44°$) except for the September 18 measurements at 40°. This discrepancy may be due to atmospheric attenuation. At the extremes of the incidence-angle range the deviation is less than 0.5 dB. However, due to the short lifetime of SEASAT (99 days, July-October), further research is needed to determine if any seasonal effects exist. The values of the mean σ^o for a particular time of day were compared over numerous flight lines to test for regional effects. No consistent discrepancies were observed over the rain forest. As a result of these tests, the entire SEASAT rain-forest data set was analyzed as a unit.

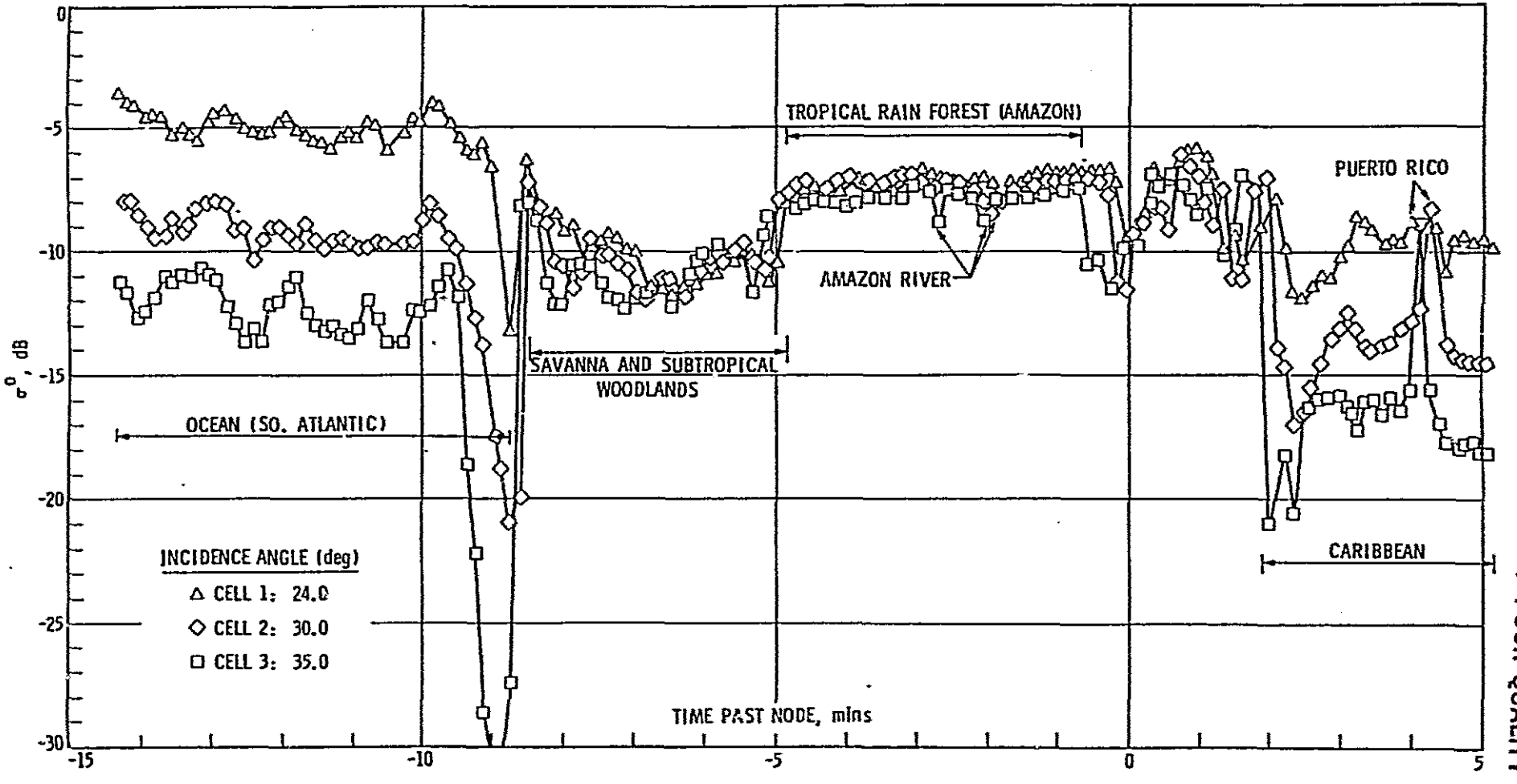

FIGURE 6: σ^o Time History for Rev 952; V-polarization; Cells 1,2,3

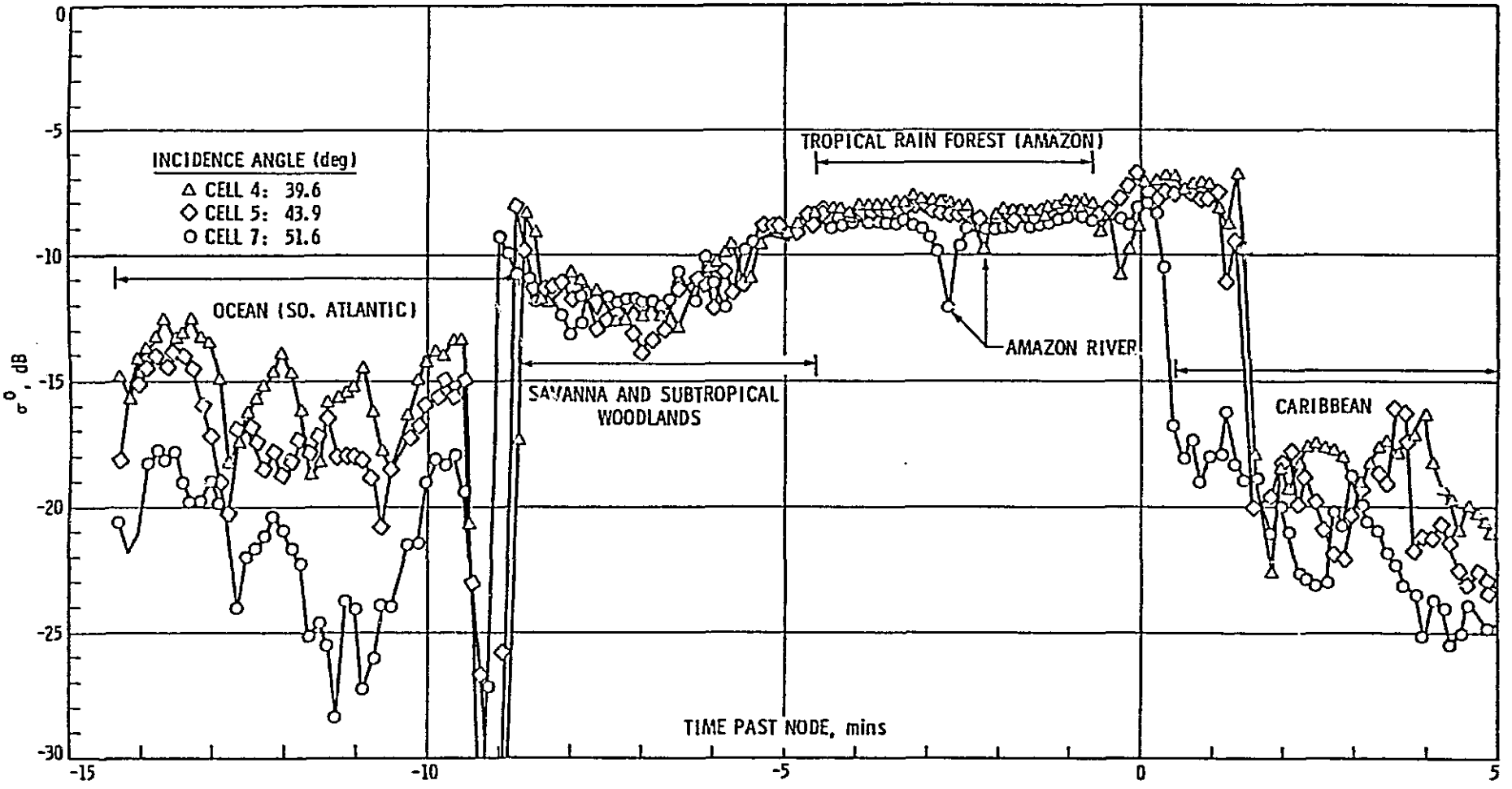

FIGURE 7: σ^o Time History for Rev 952; V-polarization; Cells 4,5,7

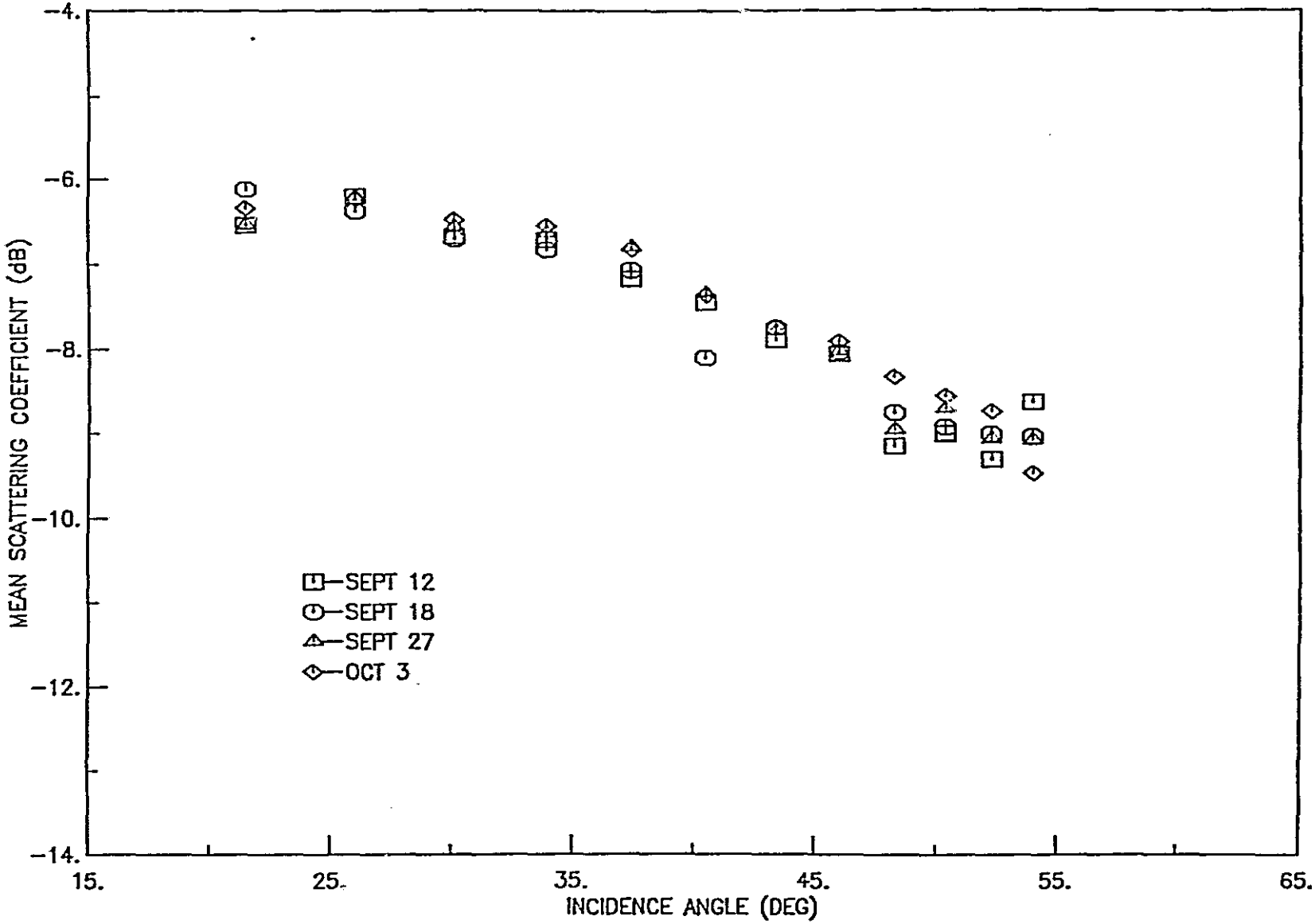

FIGURE 8: Target Stability During SEASAT Mission

4.3 Incidence Angle Dependence and Diurnal Variation

The SASS made measurements over the Amazon rain forest twice daily. During the early part of the mission, the Brazil crossings were between 0500 and 0630 (local time at center of area) and between 1630 and 1830. During the last month of the SEASAT mission, the crossings took place between 0900 and 1200 and between 2100 and 2400. For the subsequent analyses the data were binned by polarization, beam, incidence angle and time of day. Mean values and standard deviations of σ^o were computed for each of these bins.

Plots and regressions of mean σ^o versus incidence angle were made for each beam to describe the small incidence-angle dependence observed in the time histories. The sample sizes for estimation of the means varied approximately from 10 to 100 measurements. Figure 9 shows the results for Beam 4, vertical polarization. The late-morning and nighttime data agree well. The results from Beams 1 and 2 indicate that the late-afternoon measurements were also consistent with the late-morning and nighttime data. On the other hand, the early-morning measurements were from 0.5 to 1.0 dB higher than data at the other times of day.

As can be clearly seen from Figure 9, the basic angular trend is adequately modeled by the equation

$$\sigma^o_{(dB)} = a\theta + b \qquad (3)$$

where θ is the incidence angle. Typical values for the incidence angle coefficient a, as determined from regression analysis, ranged from 0.077 to 0.159 dB/deg depending on beam and time of day.

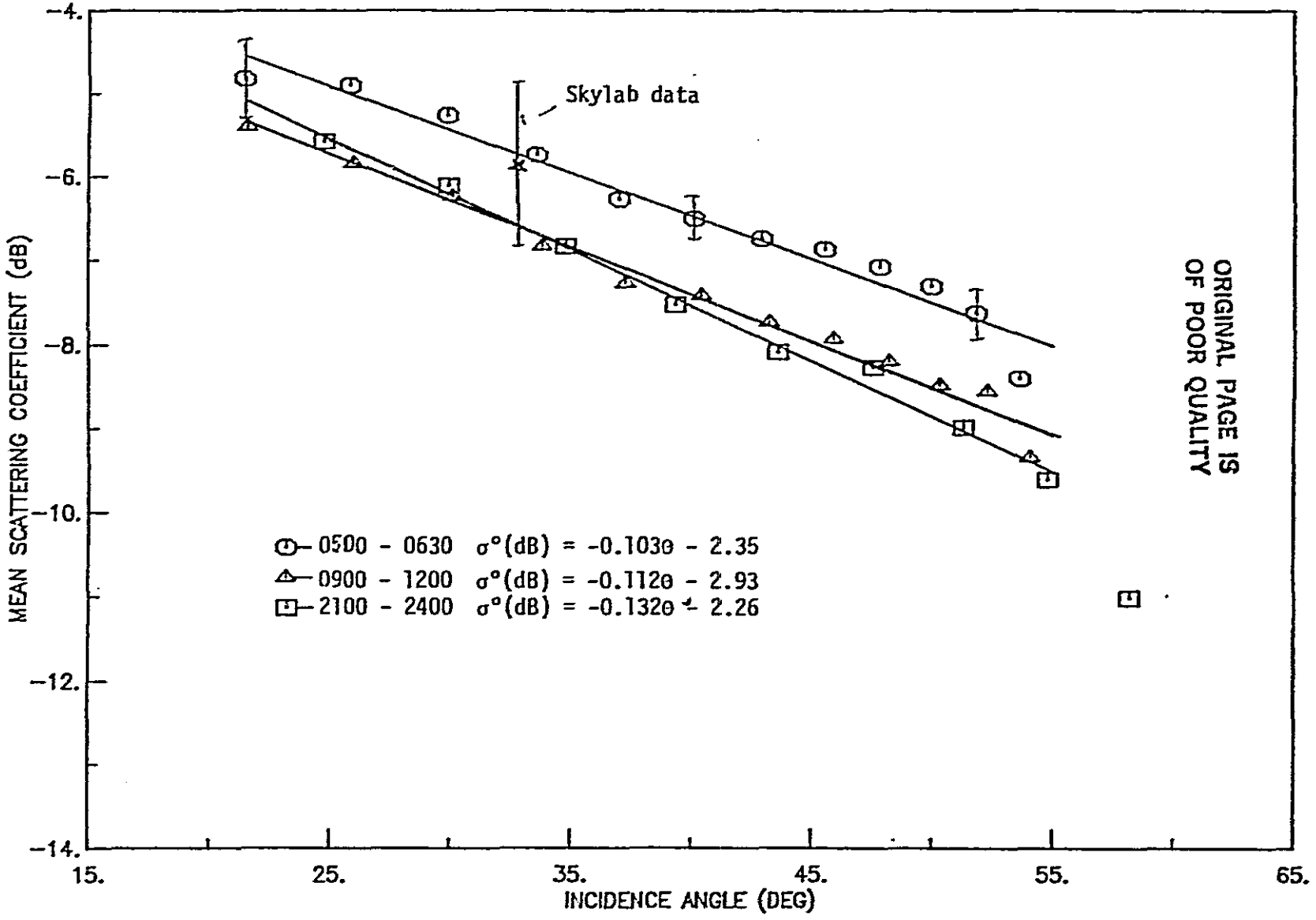

FIGURE 9: Mean σ° vs Incidence Angle; Beam 4; V-polarization

Equation (3) may be rewritten as

$$\sigma^{o}_{(real)} = K^{-\theta/\theta_o} \qquad (4)$$

where:

$$K = e^{\frac{b}{10} \ln 10}$$

$$\theta_o = -\frac{10}{a \ln 10}$$

Table 2 gives a complete summary of the values of a, b, K, θ_o determined by regression using (3)*. From the summary in Table 2 some obvious differences are observed between beams. The data appear to be most consistent in the incidence angle range of 30° - 50°. The four SASS antennas had been cross-calibrated using the eleven Brazil passes available to NASA Langley scientists soon after the SEASAT mission [4]. Good agreement was achieved in the mid-angular range. The remaining differences highlight the need for the more sophisticated cross-calibration algorithm (using all of the SEASAT passes) developed here.

The value of σ^o estimated from the regression fit agrees well with the reported SKYLAB results. The SASS, however, shows much less deviation about the mean. Bars have been drawn on Figure 9 to show the scatter in the measurements. At incidence angles near the nominal pointing angle of 44°, the standard deviations ranged from 0.1 to 0.2 dB. At the extremes of the incidence angle range the standard deviations ranged from 0.3 to 0.6 dB. This

*Both unweighted regressions and regressions weighted by number of cases were tried. Weighted regression results are reported here because they take into account the higher density of measurements in the angular region of greatest measurement accuracy. In most cases the differences in the "a" coefficients between the weighted and unweighted regression were within the errors of the estimated coefficients.

TABLE 2
Regression Parameters for the
Incidence Angle Response of SASS Data over Brazil

Model: $\sigma^{o}_{(dB)} = a\theta + b$

$\sigma^{o}(real) = K\, e^{-\theta/\theta_o}$, where K, θ_o are determined from a, b.

Beam #	Time of day*	a	b	$R^2 \times 100$%	K	θ_o	Number of cases
1	1	-0.129	-1.75	98	0.669	33.67	72
	2	-0.158	-1.71	99	0.764	27.41	246
	3	-0.112	-2.85	96	0.519	38.68	543
	4	-0.096	-3.69	94	0.428	45.30	551
2	1	-0.077	-3.62	96	0.435	56.31	166
	2	-0.089	-4.08	92	0.391	49.00	518
	3	-0.135	-1.98	98	0.663	32.17	442
	4	-0.155	-1.11	97	0.774	28.09	437
3	1	-0.148	-0.58	93	0.874	29.30	103
	2	-0.156	-1.15	96	0.767	27.91	603
	3+	------	-----	--	-----	-----	---
	4	-0.078	-4.37	96	0.366	55.61	836
4	1	-0.103	-2.35	97	0.582	42.29	140
	2	-0.112	-2.93	97	0.510	38.65	589
	3+	------	-----	--	-----	-----	---
	4	-0.132	-2.26	99	0.595	32.95	538

*Time Code: 1 = 0500-0630
2 = 0900-1200
3 = 1630-1830
4 = 2100-2400

+No data available

%Squared multiple correlation coefficient

increase in the standard deviation is probably due to a decrease in measurement precision caused by weaker signals at angles well away from the peak antenna gain, and also may be caused by small beam-pointing-angle errors that have more importance where the antenna gain varies more rapidly with angle.

The regression equations determined from the data were used to estimate values of σ^0 at 40° incidence angle which are plotted in Figure 10 as a function of time of day for Beam 2. The early morning return is 0.6 - 0.9 dB higher than at the other times of day. Table 3 summarizes these estimates for all of the beams. When this effect was first noted in the original analysis of the first 11 passes, all of the data had been screened using GOES imagery to eliminate cases containing significant cloud cover. In the present analysis the data were not screened. However, since this was the dry season few of the measurements should have been corrupted.

Initially it was believed that, because of the random orientation of the scatterers in the uniformly vegetated rain forest, the values of σ^0 would be insensitive to polarization. While most of the measurements were vertically polarized, enough horizontal polarization data were taken to allow a comparison. On Figure 11 are plots of both V-pol and H-pol data for Beam 1. As expected the results appear to be insensitive to polarization.

No noticeable azimuthal-angle variation was observed in the rain-forest data. This isotropy can be demonstrated by comparing the 0900 - 1200 V-pol data from Beam 2 and Beam 4. While the beams differ 180° in azimuth, the measurements show agreement within 0.1 - 0.2 dB. This may be seen by overlaying Figures 9 and 11.

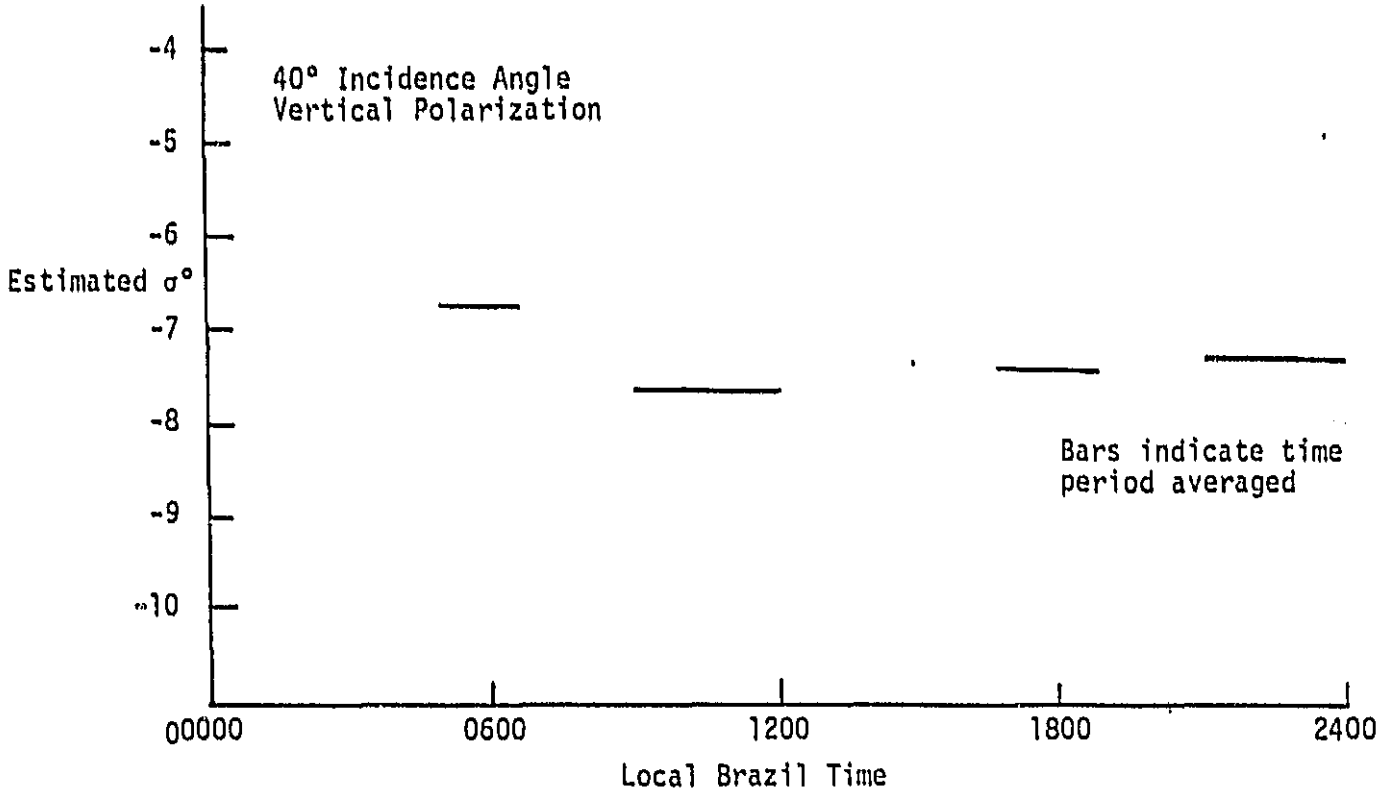

FIGURE 10: Estimated σ° From Regression Fit

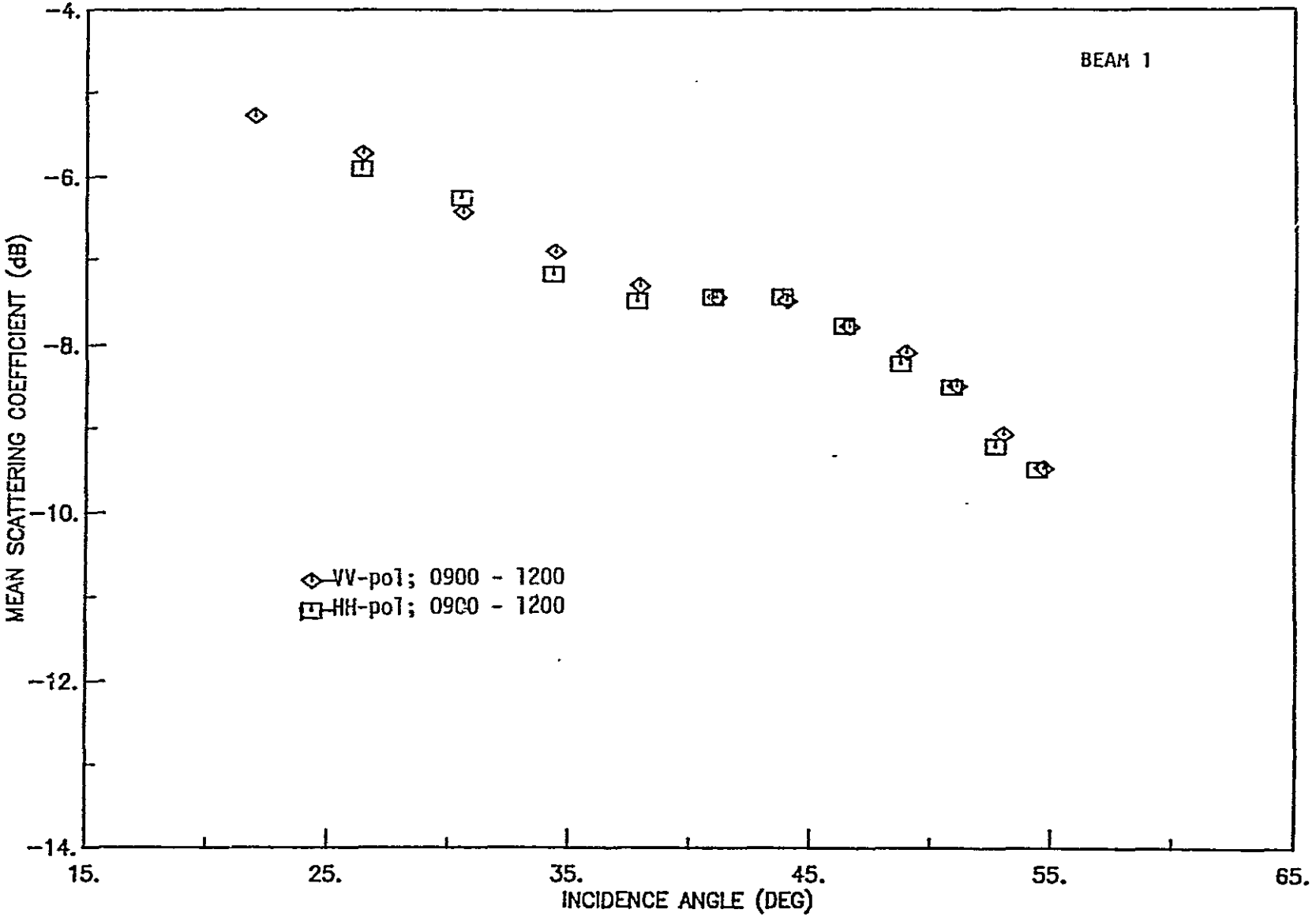

FIGURE 11: Comparison of VV-pol and HH-pol Data

TABLE 3
Summary of Diurnal Effect at 40° Incidence Angle
Vertical Polarization

Time of Day	ESTIMATED SCATTERING COEFFICIENT (dB)				Average for All Beams
	Beam 1	Beam 2	Beam 3	Beam 4	
0500 - 0630	-6.91	-6.70	-6.34	-6.47	-6.60
0900 - 1200	-7.49	-7.62	-7.39	-7.41	-7.48
1630 - 1830	-7.33	-7.40	-----	-----	-7.36
2100 - 2400	-7.53	-7.31	-7.49	-7.54	-7.47

4.4 SEASAT Summary

The data obtained from SEASAT-1 have shown the potential of the Amazon rain forest for use as a standard target. Since the diurnal effects appear to be limited to early morning, data from other times of day could all be used together to build a data base for calibration. The small scatter (0.1 - 0.6 dB) in the mean values of σ^o indicates the remarkable stability of this region and hence its usefulness as a standard target. A basic characterization of the incidence-angle dependence can be made using a simple straight-line model of $\sigma^o_{(dB)}$ vs θ.

The differences between the regression coefficients shown in Table 2 for the different beams cannot be due to actual σ^o differences because Beams 1 and 2 covered the same area, as did Beams 3 and 4. Hence these differences must be in antenna patterns or in pointing-angle differences. This points out the need for use of such a "standard target" in future multibeam scatterometers.

5.0 DEVELOPMENT OF OFF-NADIR ANTENNA BIAS CORRECTIONS FOR NOSS

5.1 Description of NOSS Scatterometer System

The NOSS Scatterometer System (SCATT) design is for a second generation fan-beam scatterometer using experience gained from SEASAT (Section 4.1). Figure 12 shows the proposed SCATT ground-track coverage. Besides the four beams used in SASS, two antennas are pointed at 65° from the satellite orbit plane to aid in wind-direction alias removal. All of the antennas are dual-polarized (V and H). The SCATT instrument transmits a 100-watt 14.0-GHz signal. The backscattered signal is Doppler filtered into 60 resolution cells with each cell approximately 10 km x 10 km. The off-nadir bias correction algorithm is to be applied to the outermost 50 Doppler cells of each beam.

5.2 Development of Maximum Likelihood (ML) Algorithms to Estimate Off-Nadir Bias Parameters

During SEASAT analysis, Brazilian rain-forest data were first used to correct for antenna biases in the off-nadir cells. Estimates for relative bias and pointing angle were determined by comparing data from a limited number of passes. For NOSS a formalized algorithm was desired to allow automation of the estimation of these parameters by using all available SCATT rain-forest data. The next subsection (5.2.1) describes in detail the derivation of a maximum likelihood (ML) approach to estimate relative bias and pointing angle.* Once pointing angle is determined, a ML technique may be used periodically to re-estimate relative bias. This algorithm is described in Section 5.2.2.

---

*This ML approach is an adaptation of the approach used in the SEASAT Wind Vector Algorithm developed by F.J. Wentz (Remote Sensing Systems, Inc.).

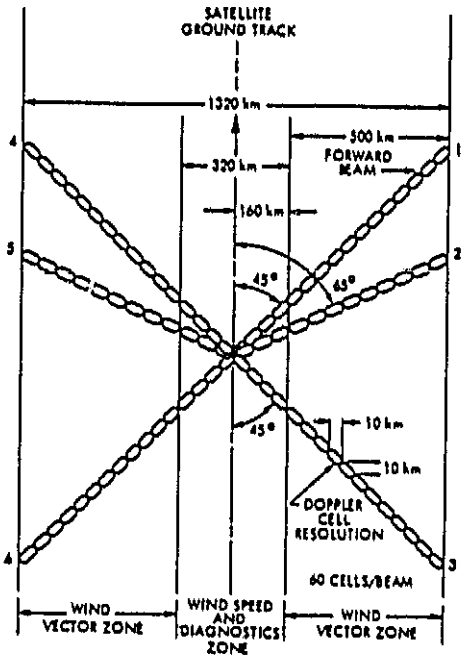

FIGURE 12: Proposed NOSS Footprint

5.2.1 Relative Bias and Pointing Angle Estimation

For an operational system the radar parameters, P_T and G_0 in equations (1) and (2) are carefully specified in the design. The relative antenna gain, $\frac{G}{G_0}$, is determined from pre-launch antenna pattern measurements and the specified pointing angle, θ_p. However, as was observed with the SASS, the actual values for P_T, G_0 and θ_p after launch can differ from the specifications [4].

Effects of these differences can be seen by writing equation (1) for both the designed and actual specifications of P_T, G_0, θ_p and the corresponding σ^o inferred from equation (2).

$$P_R = \frac{P_{DT}\lambda^2 G_{D0}[G/G_0(\theta_{DP})]^2 \sigma^o_D A}{(4\pi)^3 R^4}$$

where the subscript D refers to the designed values.

$$P_R = \frac{P_{AT}\lambda^2 G_{A0}^2[G/G_0(\theta_{AP})]^2 \sigma^o_A A}{(4\pi)^3 R^4}$$

where the subscript A refers to actual values.

Equating the above expressions and solving for σ^o_D in terms of σ^o_A yields

$$\sigma^o_D = \frac{\alpha[G/G_0\ (\theta_{AP})]^2 \sigma^o_A}{[G/G_0\ (\theta_{DP})]^2} \qquad (5)$$

where $\alpha \triangleq$ relative bias $= \dfrac{P_{AT}\ G_{A0}^2}{P_{DT}\ G_{D0}^2}$

By substituting a standard reference target, σ^o_S, for the value of σ^o_A, the relationship in equation (5) can be used to estimate the relative bias, α, and the actual pointing angle θ_{AP}. Since the measurements, σ^o_D, are noisy,

maximum-likelihood estimation is used to determine α and θ_{A^P}.

Formulation of the maximum-likelihood estimation may be given as: a vector of noisy observations, $\underset{\sim}{z}$, exists which depends probabilistically on a parameter of interest, B. The M.L. estimate of B is then given by the condition

$$f_{\underset{\sim}{z}/B}(\underset{\sim}{z}/B)\Big|_{B=\hat{b}_{ML}(z)} = \text{maximum} \tag{6}$$

where:

$f_{\underset{\sim}{z}/B}$ is the joint conditional probability density function.

$\hat{b}_{ML}(z)$ is the maximum-likelihood estimate of B.

This approach can be applied to estimate α and θ_{A^P} with the following assumptions:

(1) Radar measurements are independent and may be described as a Gaussian process

(2) The noisy observations, $\underset{\sim}{z}$, are the parameter σ_D^o

(3) The parameter of interest, B, is given by the relation:

$$\frac{\alpha\,[G/G_0\,(\theta_{A^P})]^2}{[G/G_0\,(\theta_{D^P})]^2}\;\sigma_S^o = B(\alpha\,\theta_{A^P})$$

(4) $G/G_0(\theta_p)$ is known from pre-launch measurements.

Applying the above conditions, the conditional probability in expression (6) may be re-written as:

$$f_{\underset{\sim}{\sigma}^o/B}\left[\{\sigma^o_{\ell D};\ \ell = 1,N\}/B(\alpha,\theta_{A^p})\right] = \frac{\prod_{\ell=1}^{N} e^{-[\sigma^o_{\ell D} - B(\alpha,\theta_{A^p})]^2/2(\Delta\sigma^o_D)^2}}{\eta} \tag{7}$$

where:

$$\eta = \prod_{\ell=1}^{N} \sqrt{2\pi(\Delta\sigma^o_D)^2}$$

Since the purpose is to select values of $\hat{\alpha},\hat{\theta}_{A^p}$ that maximize expression (7), two simplifications can be made. First, the quantity, η, may be ignored since it is not a function of the parameters α,θ_{A^p}. Second, the logarithm of the likelihood function may be maximized, since the same values $\hat{\alpha},\hat{\theta}_p$ will maximize both the likelihood function and the log-likelihood function. Therefore, the condition to satisfy is:

$$-1/2 \sum_{\ell=1}^{N} (\sigma^o_{\ell D} - B)^2 = \max \tag{8}$$

where $B = B(\alpha,\theta_{A^p})$.

Since the function $G/G_0(\theta_p)$ is stored as a look-up table and very difficult to express analytically, the log-likelihood expression in (8) is maximized in two steps. First a migrating search is performed to approximately center a 3 x 3 matrix about the solution. Then the maximum of a bivariate interpolating polynomial fit to points on this matrix is found to obtain $\hat{\alpha},\hat{\theta}_p$.

The search is done by defining a log-likelihood matrix, $g_{i,j}$, as follows:

$$g_{i,j} = -1/2 \sum_{\ell=1}^{N} [\sigma^o_{\ell D} - B(\alpha_i,\theta_{jp})]^2 \tag{9}$$

where:

$$\alpha_I = \alpha_o + I\Delta\alpha;\ I = -1,0,1$$

$$\theta_{Jp} = \theta_{op} + J\Delta\theta_p;\ J = -1,0,1$$

Since the actual values for P_T and G_0 should be reasonably close to the design specifications, initially α_o is chosen to be 1.0. Similarly, the design-specified pointing angle, θ_{DP}, is chosen for the initial value of θ_{op}. Reasonable values for $\Delta\alpha,\Delta\theta_p$ appear to be 0.2 and 1.0 respectively. The values for $g_{I,J}$ are then compared to find the maximum. If the center point, $g_{0,0}$, is not the maximum, a new matrix is formed as follows:

$$\alpha_I = \alpha_{max} + I\ \Delta\alpha;\ I = -1,0,1$$

$$\theta_{Jp} = \theta_{p_{max}} + J\ \Delta\theta_p;\ J = -1,0,1$$

where:

$\alpha_{max},\theta_{p_{max}}$ are the α_I,θ_{Jp} corresponding to the maximum of the previous matrix.

Searching continues until a matrix is formed which has the maximum at the center.

Estimates for relative bias, $\hat{\alpha}$, and actual pointing angle, $\hat{\theta}_p$, are found by fitting a bi-variate, quadratic interpolating polynomial to the values of $g_{I,J}$. Values of $\hat{\alpha}$ and $\hat{\theta}_p$ which maximize the polynomial are then determined analytically. The interpolating polynomial is of the form:

$$g(\hat{\alpha},\hat{\theta}_p) = a\beta^2 + b\beta + c\gamma^2 + d\gamma + e\beta\gamma + f \qquad (10)$$

where:

$$\beta = (\alpha-\alpha_0\ )/\Delta\alpha$$

$$\gamma = (\hat{\theta}_p-\theta_{0_p}\ )/\Delta\theta_p$$

$$a = \frac{g_{1,0}}{2} - g_{0,0} + \frac{g_{1,0}}{2}$$

$$b = \frac{-g_{-1,0}}{2} + \frac{g_{1,0}}{2}$$

$$c = \frac{g_{0,-1}}{2} - g_{0,0} + \frac{g_{0,1}}{2}$$

$$d = \frac{-g_{0,-1}}{2} + \frac{g_{0,1}}{2}$$

$$e = g_{0,0} - g_{1,0} - g_{0,1} + g_{1,1}$$

$$f = g_{0,0}$$

where $g_{I,J}$ are the values of the likelihood matrix.

The maximum is found by taking the partial derivatives of the interpolating polynomial and setting them equal to zero. When the resultant equations are solved for $\hat{\alpha}$ and $\hat{\theta}_p$ we get

$$\hat{\alpha}_{ML} = \alpha_0 + \frac{\Delta\alpha(ed - 2bc)}{4ac - e^2} \tag{11a}$$

$$\hat{\theta}_{p_{ML}} = \theta_{p_0} + \frac{\Delta\theta_p(be - 2ad)}{4ac - e^2} \tag{11b}$$

where a,b,c,d,e are defined as above.

5.2.2 Long-Term Monitoring of Relative Bias

Periodic estimates of the relative bias during the mission will provide a means to correct for long-term drifts in transmitter power. If the pointing angle is not expected to change once $\hat{\theta}_p$ is determined, a simplified version of the algorithm in Section 5.2.1 may be used to estimate relative bias.

In this case the parameter of interest contains only one unknown, the relative bias α. The same procedure followed in Section 5.2.1 is used to solve this one-parameter case with a likelihood vector, g_l, replacing the matrix $g_{l,J}$. The vector is defined as:

$$g_l = -\frac{1}{2} \sum_{\ell=1}^{N} [\sigma^o_{\ell D} - \alpha_l \sigma^o_S]^2; \quad l = -1,0,1 \tag{12}$$

where:

$\sigma^o_{\ell D}$ = the NOSS SCATT measurement

σ^o_S = the standard target

$\alpha_l = \alpha_0 + l\Delta\alpha$

α_0 = previously determined relative bias

Vector g_l is then fitted with a quadratic interpolating polynomial of the form:

$$g(\hat{\alpha}) = r\beta^2 + s\beta + t \tag{13}$$

where:

$$\beta = \frac{(\hat{\alpha} - \alpha_0)}{\Delta\alpha}$$

$$r = \frac{g_{-1}}{2} - g_0 + \frac{g_1}{2}$$

$$s = -\frac{g_{-1}}{2} + \frac{g_1}{2}$$

$$t = g_0$$

g_l = the values of the vector calculated in equation (12).

By differentiating equation (13) and setting the result equal to zero, the maximum likelihood value of $\hat{\alpha}$ is found as:

$$\hat{\alpha}_{ML} = \alpha_0 - \frac{s\Delta\alpha}{2r} = \alpha_0 - \Delta\alpha\left(\frac{g_1 - g_{-1}}{g_{-1} - 2g_0 + g_1}\right)$$

5.3 Implementation of Off-Nadir Bias Algorithm for NOSS SCATT

The flow chart in Figure 13 shows the relationship between the off-nadir bias algorithm and SCATT data processing. Earth-located σ^o data are screened to locate data over the Amazon rain forest. Then the Amazon map described in Section 3.0 is used to remove measurements that include either the Amazon river or one of its principal tributaries. Remaining rain-forest data are then supplied to the off-nadir bias algorithm.

Actual estimates of the relative bias and pointing angle are performed off-line from the main SCATT processing. This is necessary for two reasons: first, Brazil passes for several days are needed to create a sufficient data base for estimation; second, considerable human interaction and evaluation is needed to interpret the results.

Figure 14 shows a flow chart of the processing required in the off-nadir bias algorithm. Inputs to the algorithms are the SCATT σ^o data from the rain forest and the corresponding brightness temperatures T_B measured by the Large Antenna Multichannel Microwave Radiometer (LAMMR). Co-located LAMMR data are used to flag and remove potential rain-corrupted SCATT measurements. A data base is then created for use with the maximum-likelihood procedure described in Section 5.2. Estimates for relative bias and antenna pointing angle are computed for every combination of beam, cell and polarization. Approximate error bounds are determined using the results of several estimations. The following subsections describe in more detail the processing required.

5.3.1 Co-Location of SCATT and LAMMR

To use LAMMR 37 GHz data to flag rain-corrupted SCATT measurements, T_B measurements must be co-located with individual SCATT σ^o measurements.

ORIGINAL PAGE IS
OF POOR QUALITY

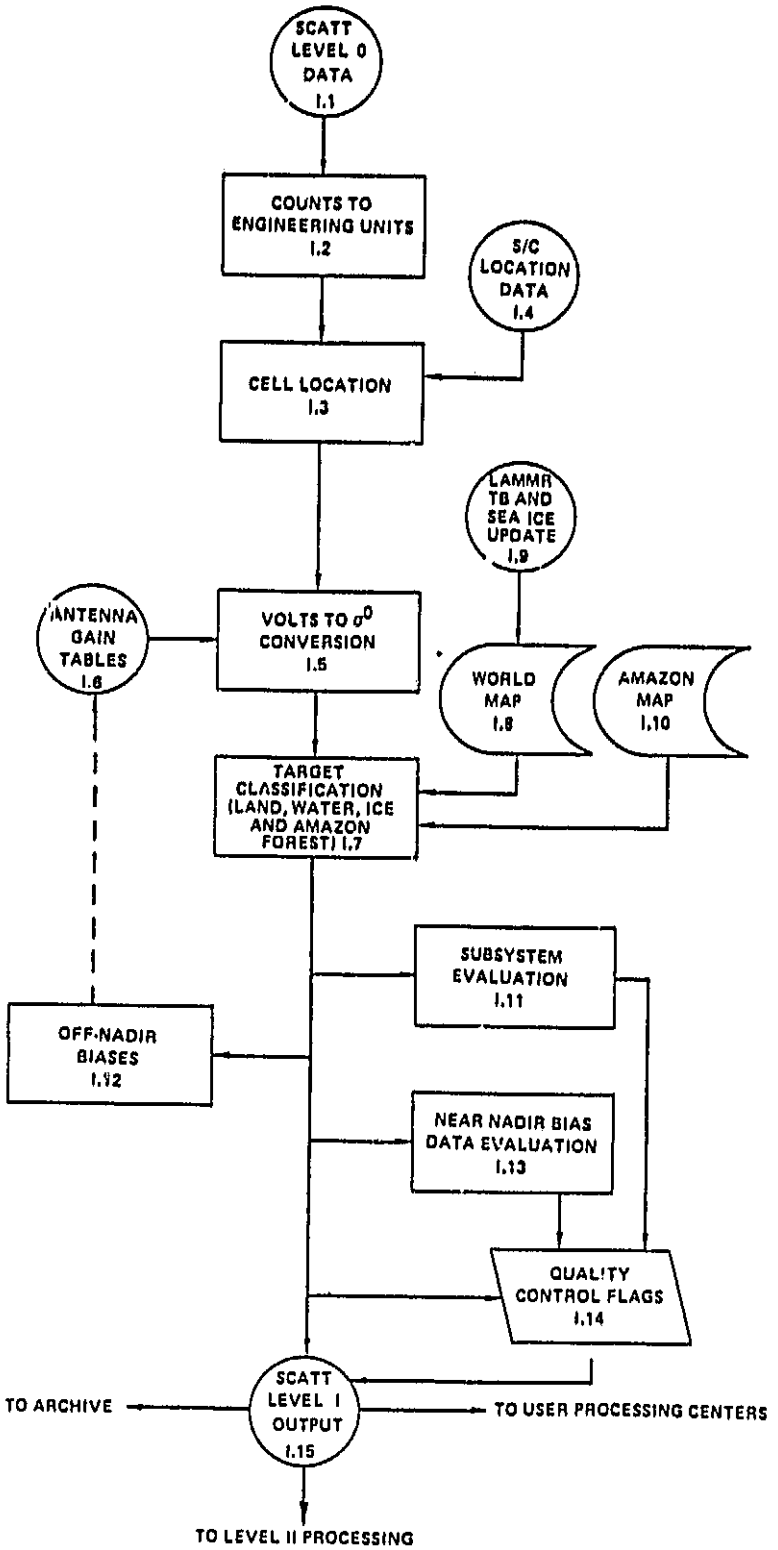

FIGURE 13: Proposed Processing of NOSS Scatterometer (SCATT) Data to Obtain σ^o

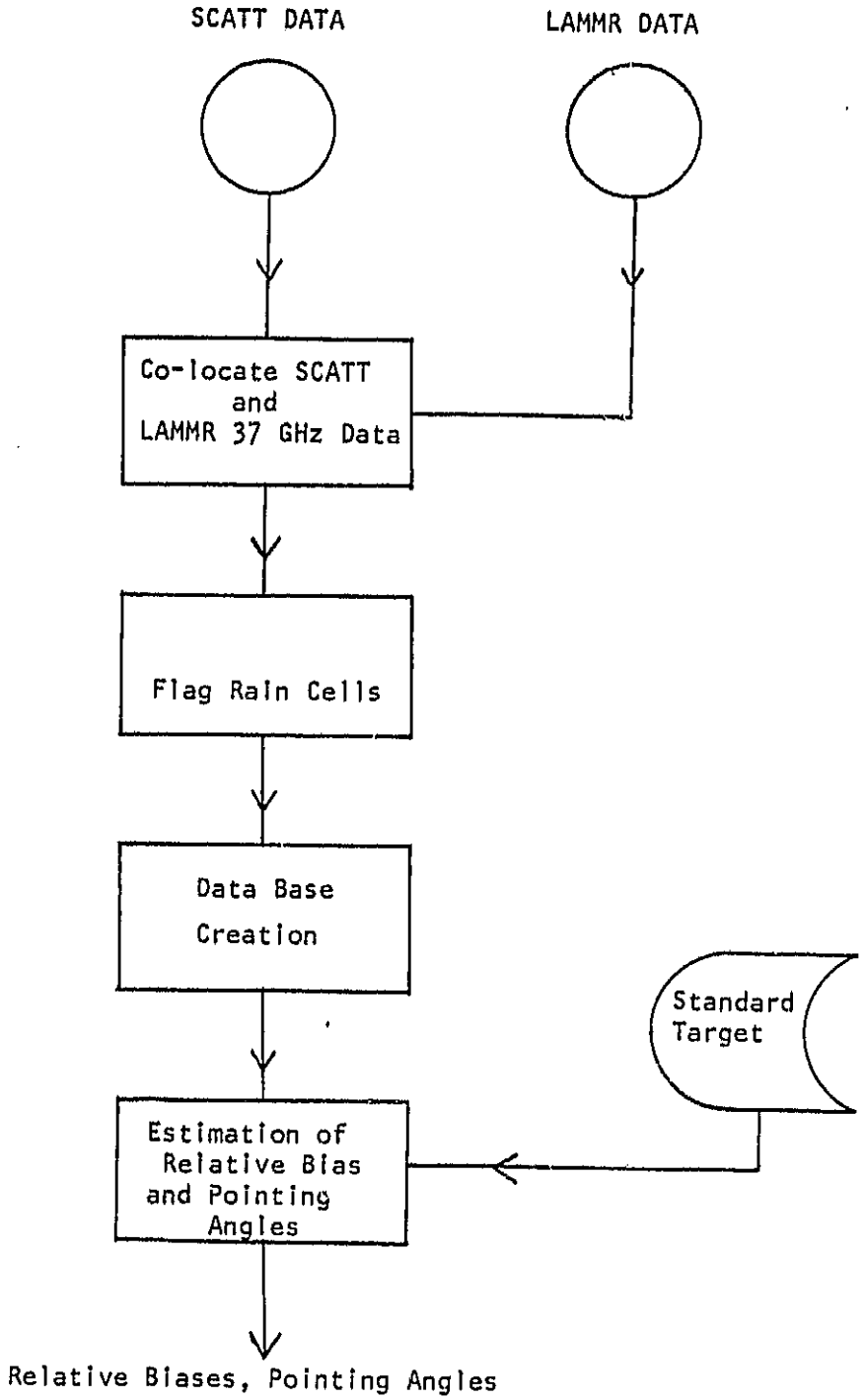

FIGURE 14: Processing Required for Off-Nadir Bias Correction

The input data streams for both SCATT and LAMMR are assumed to be gridded into 50 km blocks and assigned a set of coordinates (i,j). Co-location is accomplished by: first, sorting both LAMMR T_B's and SCATT σ^o's independently by grid coordinates; second, for each coordinate pair (i,j) containing SCATT data the corresponding LAMMR grid point is located. Within the 50 km grid each SCATT cell is matched with the closest LAMMR cell.

5.3.2 Flagging Rain Cells

Co-located LAMMR 37 GHz T_B's are used to flag potential rain-corrupted SCATT cells. The brightness temperature of the Brazilian rain forest is very high due to high emissivity and surface temperature. However, in the presence of rain only the top portion of the rain cloud and not the forest is seen. Hence it is believed that the temperature measured should be lower when rain occurs than in clear sky conditions. Rain flags will be set whenever the measured temperature falls below a fixed cut-off temperature, T_{cut}.

Figure 15 shows the form of the 37 GHz brightness temperature histogram expected from the Amazon rain forest. The lobe at the lower brightness temperature corresponds to measurements made in rain conditions, while the lobe at higher brightness temperature corresponds to clear-sky conditions. A preliminary value for T_{cut} may possible be made from SEASAT radiometer measurements. However, it will be important to make a number of histograms with LAMMR data to confirm the assumed distribution shown in Figure 15 and to properly set T_{cut}.

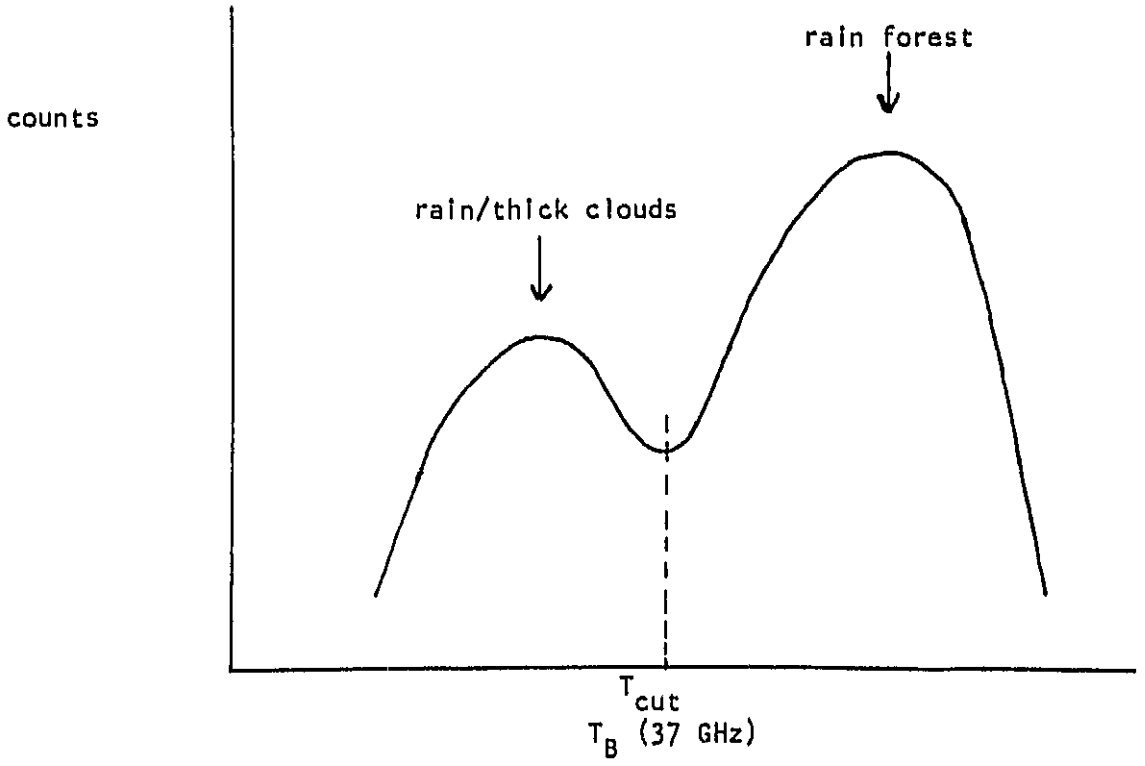

FIGURE 15: Nature of Expected Amazon T_B Distribution

5.3.3 Data Base Creation

Due to the large volume of data produced by the SCATT, estimation of relative bias and pointing angle is performed by using mean σ^0 values computed for each pass over Brazil. Individual clear-sky SCATT measurements are grouped by beam, cell number and polarization. At the end of each Brazil pass the mean value, standard deviation, and average incidence angle is computed for each group containing more than twenty measurements. These estimates are also binned by beam, cell number and polarization. Estimation of relative bias and pointing angle takes place when each mean value bin has data from at least 10 passes. Since the bins will fill at different rates depending on the location of the satellite subtrack, provision is made to store up to 20 values in each.

5.3.4 Standard Target Creation

The maximum likelihood procedure described in Section 5.2 requires a standard target, $\sigma_S^0(\theta)$, defined over the entire off-nadir incidence angle range. Determination of σ_S^0 will require consistent human evaluation and decision.

Initially plots and regressions of the mean value of σ^0 versus incidence angle will be made from the data base described above. These plots and regressions will be compared with SEASAT results described in Section 4.0 and Appendix B. If there is good comparison in trend, the SEASAT model, $\sigma^0_{dB} = a\theta + b$, will be adopted with an appropriate level shift. If the trend of the SCATT data is significantly different, a new model determined from the analysis of several passes may be used. The final procedure used in creating the standard target will be determined once the initial comparisons are made.

5.3.5 Relative Bias and Pointing Angle Estimation

Early in a future mission with the NOSS design will be the implementation of the ML technique to determine both relative bias and pointing angle described in Section 5.2.2. Once a suitable value for pointing angle is determined for each beam, the simplified algorithm described in Section 5.2.3 may be used to monitor long-range transmitter drift. Both of these algorithms can be implemented using the same inputs so switching between algorithms should be trivial.

In this implementation the noisy data, $\sigma^o_{\ell D}$ in equations (8) and (12) are the mean values stored in the data base (Section 5.3.3). Separate estimates will be made for each combination of beam, cell and polarization. Repeated estimates should be made using subsequent data. Final estimates and bounds may be calculated by computing the means and standard deviations.

6.0 CONCLUSIONS AND FUTURE RESEARCH

Detailed analysis of SEASAT scatterometer data has confirmed the suitability of the Amazon rain forest for use as a standard calibration target. A simple straight line model for incidence angle variation appears to be quite adequate. Useful approximations for the model parameters may be determined from the SASS data. The accuracy of these approximations is limited by remaining biases between SASS antennas and the lack of independent rain-forest measurements for absolute calibration.

Maximum-likelihood estimation algorithms have been developed to correct off-nadir antenna biases for spaceborne scatterometers by utilizing rain-forest data. Application of those algorithms for the proposed NOSS scatterometer was straight-forward. Presumably these techniques could be adapted easily for calibrating other future systems.

Three important areas of research need to be undertaken to extend the usefulness of Amazon rain forest data to correct off-nadir antenna biases. First, measurements must be made throughout the year to determine the existence of any seasonal effects. The SEASAT measurements were made during only the dry season. Second, research needs to be done to confirm the proposed algorithm to screen out data corrupted by thick clouds and rain. The multifrequency radiometer measurements made with the NIMBUS 7 satellite could potentially contribute valuable information in both of these areas. Third, a calibration program using aircraft overflights is needed to better determine the absolute value of σ^o.

REFERENCES

[1] Sobti, A., R.K. Moore and S.T. Ulaby, "Backscatter Response at 13.9 GHz for Major Terrain Types As Seen From Orbit," Remote Sensing Laboratory Technical Report 243-4, August 1975. University of Kansas Center for Research, Inc., Lawrence, Kansas 66045.

[2] Sobti, A. and E.C. Davidson, "Microwave Scattering Measurements Over Brazil at 13.9 GHz," Remote Sensing Laboratory Technical Report 243-11, September 1975. University of Kansas Center for Research, Inc., Lawrence, Kansas 66045.

[3] Grantham, W.L., E.M. Bracalente, W.L. Jones, J.H. Shrader, L.C. Schroeder and J.L. Mitchell, "An Operational Satellite Scatterometer for Wind Vector Measurements over the Oceans," NASA TMS 72676, March 1975.

[4] Bracalente, E.M., D.H. Boggs, W.L. Grantham and J.L. Sweet, "The SASS Scattering Coefficient σ^o Algorithm," IEEE Journal of Oceanic Engineering, vol. OE-5, no. 2, April 1980, pp. 145-149.

APPENDIX A

```
CBRZLND                  LAND/WATER ROUTINE FOR BRZILIAN RAIN FOREST     00000010
C     .                                                                  00000020
      SUBROUTINE LDBRZL                                                  00000030
C                                                                        00000040
C     PURPOSE                                                            00000050
C                                                                        00000060
C         THIS ROUTINE LOADS THE LAND WATERMAP                           00000070
C                                                                        00000080
       INTEGER ARRAY(6,10,64),CODE                                       00000090
       REAL GLAT(6)/2.,0.,-2.,-4.,-6.,-8./                               00000100
       REAL GLON(10)/74.,72.,70.,68.,66.,64.,                            00000110
     &   62.,60.,58.,56./                                                00000120
       REAL LAT,LONG                                                     00000130
C                                                                        00000140
C                              READ LAND/WATER MAP                       00000150
C                                                                        00000160
       DO 10 I=1,6                                                       00000170
       DO 10 J=1,10                                                      00000180
       READ(01,900) (ARRAY(I,J,K),K=1,64)                                00000190
 900   FORMAT(4X,8I8)                                                    00000200
 10    CONTINUE                                                          00000210
C                                                                        00000220
      RETURN                                                             00000230
C                                                                        00000240
      ENTRY LNDH2O(TLAT,TLONG, CODE)                                     00000250
C                                                                        00000260
C                                                                        00000270
C     PURPOSE                                                            00000280
C                                                                        00000290
C         THIS ROUTINE FETCHES A LAND/WATER CODE                         00000300
C         CORRESPONDING TO AN INPUT LATITUDE AND                         00000310
C         LONGITUDE                                                      00000320
C                                                                        00000330
C     INPUT ARGUMENTS                                                    00000340
C                                                                        00000350
C         TLAT          *          LATITUDE (DEG)                      00000360
C         TLONG         *          EAST LONGITUDE (DEG)                00000370
C                                                                        00000380
C     OUTPUT ARGUMENT                                                    00000390
C                                                                        00000400
C         CODE          *          LAND/WATER CODE                     00000410
      LAT = TLAT                                                         00000420
      LONG = TLONG                                                       00000430
C                                                                        00000440
      LONG = 360.0 - LONG                                                00000450
       ILAT = IFIX( (2.-LAT)/2. ) + 1                                    00000460
       JLON = IFIX( (74.-LONG)/2. ) + 1                                  00000470
       ITEP = IFIX( (GLAT(ILAT) - LAT)/0.25 )                            00000480
       JTEP = IFIX( (GLON(JLON) - LONG)/0.25) + 1                        00000490
       KELE = ITEP*8 + JTEP                                              00000500
       CODE = 1 + ARRAY(ILAT,JLON,KELE)                                  00000510
      RETURN                                                             00000520
       END                                                               00000530
CBRZVEG        VEGETATION CODE ROUTINE FOR BRAZILAIN AREA                00000540
C                                                                        00000550
```

```
      SUBROUTINE LDVEG                                                  00000560
C                                                                       00000570
C     PURPOSE                                                           00000580
C                                                                       00000590
C             THIS ROUTINE LOADS THE VEGETATION MAP                     00000600
C                                                                       00000610
      INTEGER VEGTBL(5,3,64),VGCODE                                     00000620
C                                                                       00000630
      REAL LAT,LNG                                                      00000640
C                                                                       00000650
      REAL VLAT(3)/2.0,-2.0,-6.0/                                       00000660
C                                                                       00000670
      REAL VLNG(5)/74.0,70.0,66.0,62.0,58.0/                            00000680
C                                                                       00000690
C                                READ VEGETATION MAP                    00000700
C                                                                       00000710
      DO 10 I = 1,5                                                     00000720
      DO 10 J = 1,3                                                     00000730
      READ(02,900)(VEGTBL(I,J,K),K=1,64)                                00000740
 10   CONTINUE                                                          00000750
 900  FORMAT(4X,8I5)                                                    00000760
C                                                                       00000770
      RETURN                                                            00000780
CVEGCD COMPUTE CORRECT VEGETATION CODE                                  00000790
C                                                                       00000800
      ENTRY VEGCD( TLAT,TLNG, VGCODE )                                  00000810
C                                                                       00000820
C     PURPOSE                                                           00000830
C                                                                       00000840
C             THIS ROUTINE INPUTS A LATITUDE AND A                      00000850
C             LONGITUDE.  WITH THESE A VEGETAION                        00000860
C             CODE IS DETERMINED                                        00000870
C                                                                       00000880
C     INPUT ARGUMENTS                                                   00000890
C                                                                       00000900
C         TLAT          *          LATITUDE (DEG)                     00000910
C         TLONG         *           EAST LONGITUDE(DEG)               00000920
C                                                                       00000930
C     OUTPUT ARGUMENT                                                   00000940
C                                                                       00000950
C         VGCODE        *          VEGETATION CODE                    00000960
C                                                                       00000970
      LAT = TLAT                                                        00000980
      LNG = TLNG                                                        00000990
C                                CONVERT TO WEST LONGITUDE              00001000
C                                                                       00001010
      LNG = 360.0 - LNG                                                 00001020
C                                                                       00001030
C                                DETERMINE VEGETATION CODE              00001040
C                                                                       00001050
      ILAT = IFIX( (2.0 - LAT) / 4.0) + 1                               00001060
      ILNG = IFIX( (74.0 - LNG) / 4.0) + 1                              00001070
C                                                                       00001080
      INDEXX = IFIX( (VLAT(ILAT) - LAT) / 0.5)                          00001090
      INDEXY = IFIX( (VLNG(ILNG) - LNG) / 0.5) + 1                      00001100
```

```
      INDEXZ = INDEXX * 8 + INDEXY                                    0000111C
C                                                                     0000112C
      VGCODE = VEGTBL(ILNG,ILAT,INDEXZ)                               0000113C
C                                                                     0000114C
      RETURN                                                          0000115C
      END                                                             0000116C
```

0	0	0	0	0	0	0	0	00000010
0	0	0	0	0	0	0	0	00000020
0	0	0	0	0	0	0	0	00000030
0	0	0	0	0	0	0	0	00000040
0	0	0	0	0	0	0	0	00000050
0	0	0	0	0	0	0	0	00000060
0	0	0	0	0	0	0	0	00000070
0	0	0	0	0	0	0	0	00000080
0	0	0	0	0	0	0	0	00000090
0	0	0	0	0	0	0	0	00000100
0	0	0	0	0	0	0	0	00000110
0	0	0	0	0	0	2	2	00000120
0	0	0	0	0	2	2	0	00000130
0	0	0	0	0	0	0	0	00000140
0	0	0	0	0	0	0	0	00000150
0	0	0	0	0	0	0	0	00000160
0	0	0	0	0	0	0	0	00000170
0	0	0	0	0	0	0	0	00000180
0	0	0	0	0	1	1	2	00000190
2	2	2	1	0	0	0	0	00000200
0	0	0	2	0	0	0	0	00000210
1	1	1	2	0	0	0	0	00000220
0	0	0	2	2	2	2	0	00000230
0	0	1	1	1	1	2	2	00000240
0	0	0	2	2	2	0	0	00000250
0	0	0	2	2	0	0	0	00000260
2	0	0	0	2	0	0	0	00000270
2	2	2	1	2	0	0	0	00000280
0	1	2	2	2	0	0	0	00000290
0	0	2	2	0	0	0	0	00000300
0	0	2	0	0	0	0	0	00000310
2	2	2	2	0	0	0	0	00000320
0	0	0	0	0	0	0	0	00000330
0	0	0	0	0	0	0	0	00000340
0	0	0	0	0	0	0	0	00000350
0	0	0	0	0	0	0	0	00000360
0	0	0	0	0	0	0	0	00000370
0	0	0	0	0	0	0	0	00000380
0	0	0	0	0	0	0	2	00000390
0	0	0	0	0	0	0	0	00000400
2	0	0	0	0	0	0	0	00000410
2	0	0	0	0	0	0	0	00000420
0	0	1	0	0	0	1	0	00000430
0	0	0	0	0	0	1	2	00000440
2	0	0	0	0	0	0	2	00000450
0	0	0	0	0	0	0	0	00000460
1	0	1	1	0	0	0	0	00000470
2	0	0	2	0	0	0	0	00000480
0	0	0	2	2	0	1	1	00000490
0	0	2	2	1	1	1	1	00000500
0	0	2	1	0	0	0	0	00000510
0	0	2	0	1	0	0	0	00000520
2	2	2	0	0	0	0	0	00000530
2	2	1	0	0	0	0	0	00000540
1	2	0	0	0	0	0	0	00000550

2	2	0	0	0	0	0	0	0000056(
3	0	0	0	0	0	0	0	0000057(
3	3	3	0	0	0	0	0	0000058(
3	3	3	3	0	0	3	3	0000059(
0	0	3	3	3	3	3	3	0000060(
0	0	0	0	0	3	3	3	0000061(
0	0	0	0	0	0	0	0	0000062(
0	0	0	0	1	0	0	1	0000063(
0	0	0	0	0	0	0	2	0000064(
0	0	3	3	3	3	3	0	0000065(
3	3	3	3	3	3	0	0	0000066(
3	3	3	3	0	0	0	0	0000067(
3	3	3	3	0	0	0	0	0000068(
0	3	3	0	2	0	0	0	0000069(
0	0	0	0	2	0	0	0	0000070(
0	0	0	0	2	0	0	0	0000071(
0	0	0	0	2	0	0	0	0000072(
0	0	0	0	0	0	0	0	000007[illegible]
0	0	0	0	0	0	0	0	0000074(
0	0	0	0	0	0	0	0	0000075(
0	0	0	0	0	0	0	0	0000076(
0	0	0	0	0	0	0	0	0000077(
0	0	0	0	0	0	0	2	0000078(
0	0	0	0	0	1	0	2	0000079(
0	0	0	0	0	2	0	2	0000080(
1	0	0	0	0	0	0	0	0000081(
2	2	0	0	0	0	2	2	0000082(
0	2	0	0	0	0	2	2	0000083(
0	0	0	0	0	0	0	0	0000084(
2	1	0	0	0	0	0	0	0000085(
2	2	0	0	0	0	0	0	0000086(
0	2	2	0	0	0	0	0	0000087(
0	0	2	2	0	0	0	0	0000088(
0	0	0	0	0	0	2	0	0000089(
0	0	0	0	0	0	2	2	0000090(
2	0	0	0	0	0	0	2	0000091(
2	2	2	2	0	0	0	2	0000092(
0	0	0	2	2	0	0	2	0000093(
0	0	0	0	2	2	2	2	0000094(
0	0	0	0	0	0	0	0	0000095(
0	0	0	0	0	0	0	0	0000096(
0	0	0	0	0	0	0	0	0000097(
0	0	0	0	0	0	0	0	0000098(
0	0	0	0	0	0	0	0	0000099(
2	1	0	0	0	0	0	0	0000100(
2	2	2	0	0	0	0	0	0000101(
2	2	2	0	0	0	0	0	0000102(
0	0	2	2	0	0	2	2	0000103(
0	0	0	2	2	2	0	0	0000104(
0	0	0	2	2	0	0	0	0000105(
0	0	0	0	0	2	2	2	0000106(
0	0	0	0	0	0	0	0	0000107(
0	0	0	0	0	0	0	0	0000108(
0	0	0	0	0	0	0	0	0000109(
0	0	0	0	0	0	0	0	0000110(

2	2	1	0	0	1	2	2	00001110
0	0	2	2	2	2	0	2	00001120
0	0	0	0	0	0	0	2	00001130
2	2	2	2	2	2	2	2	00001140
0	0	0	1	2	0	0	0	00001150
0	0	0	0	0	0	0	0	00001160
0	0	0	0	0	0	0	2	00001170
1	2	0	0	0	0	0	0	00001180
2	2	0	0	0	0	0	1	00001190
2	2	2	2	0	0	1	1	00001200
2	0	2	2	2	0	0	0	00001210
2	2	2	2	2	1	1	1	00001220
0	2	2	2	2	1	2	1	00001230
2	0	2	2	2	2	2	2	00001240
2	2	2	1	2	2	2	2	00001250
0	0	1	1	1	1	2	2	00001260
2	2	2	2	2	2	2	2	00001270
1	1	1	1	1	2	2	2	00001280
2	0	2	0	0	0	0	0	00001290
2	1	2	2	0	0	2	2	00001300
2	2	2	2	0	0	2	0	00001310
2	2	1	1	2	2	1	0	00001320
2	2	1	1	0	0	0	0	00001330
2	2	2	0	0	0	0	0	00001340
2	2	2	1	1	1	0	0	00001350
2	2	2	2	0	0	0	0	00001360
0	0	0	0	0	0	0	2	00001370
0	0	0	0	0	0	0	2	00001380
0	0	0	2	0	0	0	2	00001390
1	1	0	2	2	0	0	2	00001400
0	0	0	0	0	2	0	0	00001410
0	0	3	3	0	2	0	0	00001420
1	2	0	0	0	2	0	0	00001430
0	2	2	1	0	2	2	0	00001440
0	0	0	0	2	0	0	2	00001450
0	0	0	0	2	0	0	2	00001460
0	0	0	0	2	0	2	2	00001470
2	0	2	2	2	0	0	2	00001480
2	2	2	2	2	0	0	2	00001490
0	0	0	0	2	2	2	2	00001500
2	2	2	2	0	0	2	2	00001510
0	0	0	2	2	2	2	2	00001520
0	0	0	0	0	0	0	0	00001530
0	0	0	0	0	0	0	0	00001540
0	0	0	0	0	0	0	0	00001550
0	0	0	3	3	3	0	0	00001560
0	3	3	0	3	3	0	0	00001570
2	0	0	0	0	3	0	3	00001580
2	0	0	0	0	0	3	3	00001590
2	2	2	0	2	0	3	3	00001600
0	0	0	2	0	0	0	0	00001610
0	0	0	2	2	2	2	2	00001620
2	2	0	0	0	0	0	0	00001630
1	2	0	0	0	0	0	0	00001640
0	2	2	1	0	0	0	0	00001650

0	0	2	2	2	2	2	2	0000166
0	0	0	2	2	2	0	0	0000167
0	0	0	2	2	0	0	0	0000168
2	2	0	2	2	0	0	0	0000169
2	2	2	2	2	2	2	0	0000170
0	0	0	0	0	2	2	2	0000171
0	0	0	0	0	0	0	0	0000172
2	2	0	0	0	0	0	0	0000173
2	2	0	0	0	0	0	0	0000174
2	2	2	2	0	2	2	2	0000175
0	0	2	2	2	2	2	2	0000176
0	0	0	0	0	0	0	0	0000177
0	0	0	0	0	0	0	0	0000178
2	2	0	0	0	0	0	0	0000179
2	2	2	2	2	2	2	0	0000180
0	0	0	2	2	2	2	2	0000181
0	0	2	2	2	2	2	2	0000182
0	0	2	2	1	2	2	2	0000183
0	2	2	0	0	0	2	0	0000184
0	0	0	0	0	2	2	2	0000185
0	0	2	2	2	2	2	2	0000186
0	2	2	2	2	2	2	2	0000187
2	2	2	2	0	0	0	0	0000188
2	0	2	0	0	0	0	2	0000189
2	0	2	0	0	0	0	2	0000190
0	2	2	0	0	0	2	2	0000191
2	2	0	0	0	0	2	0	0000192
2	2	2	2	1	1	1	1	0000193
2	2	2	2	2	2	0	1	0000194
2	2	2	2	2	2	2	0	0000195
2	0	2	2	2	2	2	0	0000196
2	0	0	2	2	2	2	2	0000197
0	0	0	0	2	2	2	2	0000198
0	0	0	0	2	2	2	2	0000199
0	0	0	0	0	0	0	2	0000200
1	1	1	1	1	1	2	2	0000201
1	1	1	1	1	1	0	0	0000202
0	1	1	1	1	1	1	1	0000203
2	0	0	0	0	1	1	1	0000204
2	1	1	2	2	2	1	1	0000205
0	2	2	0	2	2	0	0	0000206
2	2	2	2	2	2	2	2	0000207
2	2	2	2	2	2	2	2	0000208
2	1	2	2	0	0	0	0	0000209
0	0	0	2	2	2	0	0	0000210
0	2	0	2	2	2	2	0	0000211
1	2	2	2	2	2	2	2	0000212
0	2	2	2	2	2	2	2	0000213
2	2	2	2	2	2	2	2	0000214
0	2	2	2	2	2	2	2	0000215
2	2	2	2	0	2	2	0	0000216
0	0	2	2	2	0	2	2	0000217
0	0	0	2	2	2	2	2	0000218
0	0	2	0	1	1	2	2	0000219
0	0	2	2	0	2	2	2	0000220

```
2 2 2 2 2 2 2 2 00002210
2 2 2 2 2 2 2 1 00002220
2 2 2 2 2 2 1 0 00002230
2 2 2 2 2 2 2 2 00002240
2 2 1 2 2 2 2 2 00002250
2 2 2 2 2 2 2 2 00002260
2 2 2 2 2 2 2 0 00002270
2 2 2 2 2 2 0 0 00002280
2 2 2 2 2 2 0 0 00002290
2 2 2 2 0 2 0 0 00002300
2 2 2 2 0 0 0 0 00002310
2 2 2 2 0 0 0 0 00002320
0 0 2 2 2 2 2 2 00002330
0 0 2 2 2 2 2 2 00002340
0 0 2 2 2 2 2 2 00002350
0 0 2 2 0 0 0 0 00002360
0 0 2 2 0 0 0 0 00002370
0 0 2 2 0 0 0 0 00002380
0 0 2 2 0 0 0 0 00002390
0 0 2 0 0 0 0 0 00002400
0 0 2 2 2 0 0 0 00002410
2 2 2 2 0 0 0 0 00002420
2 2 2 0 0 0 0 0 00002430
2 0 0 0 0 0 0 0 00002440
0 0 0 0 0 0 0 0 00002450
0 0 0 0 0 0 0 0 00002460
0 0 0 0 0 0 0 0 00002470
0 0 0 0 0 0 0 0 00002480
0 0 0 0 0 2 2 2 00002490
0 0 0 0 2 2 2 2 00002500
0 0 0 0 0 0 2 0 00002510
0 0 0 0 0 0 0 0 00002520
0 0 0 0 0 0 0 0 00002530
0 0 0 0 0 0 0 0 00002540
0 0 0 0 0 0 0 0 00002550
0 0 0 0 0 0 0 0 00002560
2 2 2 0 1 0 0 0 00002570
2 2 0 1 1 0 0 0 00002580
0 0 1 1 0 0 0 0 00002590
0 0 1 0 0 0 0 0 00002600
0 0 0 0 0 0 0 0 00002610
0 0 0 0 0 0 0 0 00002620
0 0 0 0 0 0 0 0 00002630
0 0 0 0 0 0 0 0 00002640
2 0 0 0 0 0 2 0 00002650
0 0 0 0 0 0 2 0 00002660
0 0 0 0 0 2 2 0 00002670
0 0 0 0 0 2 0 0 00002680
0 0 0 2 2 0 0 0 00002690
0 2 2 1 0 0 0 0 00002700
2 2 0 0 0 0 0 0 00002710
0 0 0 0 0 0 0 0 00002720
0 0 0 0 0 0 0 1 00002730
0 0 0 0 0 0 1 1 00002740
0 2 0 0 0 0 1 0 00002750
```

0	0	0	0	0	0	0	2	00002760
0	0	0	0	0	0	0	0	00002770
0	0	0	0	0	0	0	0	00002780
0	0	0	0	0	2	2	2	00002790
0	0	0	0	2	2	2	0	00002800
2	2	2	2	2	2	2	2	00002810
2	2	2	2	1	1	2	2	00002820
0	1	0	0	0	0	2	2	00002830
2	0	0	0	2	2	2	0	00002840
0	0	0	0	2	1	2	0	00002850
0	0	0	2	2	0	0	0	00002860
2	2	2	2	2	0	0	0	00002870
2	2	2	1	0	0	0	0	00002880
2	2	2	1	1	2	2	0	00002890
2	2	0	0	0	2	2	2	00002900
2	0	0	0	1	2	2	2	00002910
0	0	0	0	2	2	2	2	00002920
0	1	2	2	2	2	2	2	00002930
0	0	0	0	2	2	2	0	00002940
0	0	2	2	2	0	2	0	00002950
0	2	2	1	0	0	2	2	00002960
2	0	2	2	2	2	2	2	00002970
2	2	2	2	2	2	2	2	00002980
2	1	2	2	2	0	0	0	00002990
2	1	2	2	0	0	0	0	00003000
2	2	2	0	0	0	0	0	00003010
2	2	0	0	0	0	0	0	00003020
2	2	0	0	0	0	0	0	00003030
2	2	2	2	0	0	0	0	00003040
0	2	0	0	0	0	0	0	00003050
0	2	0	0	0	0	2	2	00003060
0	0	0	0	0	2	2	2	00003070
0	0	0	0	0	2	2	0	00003080
0	0	0	0	2	2	2	2	00003090
0	0	0	0	2	0	0	2	00003100
0	0	2	2	2	0	0	0	00003110
0	2	2	2	0	0	0	0	00003120
2	2	0	0	0	0	0	0	00003130
2	0	0	0	0	0	0	0	00003140
0	0	0	0	0	0	2	2	00003150
0	0	0	0	0	2	2	0	00003160
3	0	0	0	0	2	2	0	00003170
3	3	0	0	0	0	2	0	00003180
3	3	0	0	0	0	2	2	00003190
3	3	0	0	0	0	2	2	00003200
0	0	0	0	0	0	0	0	00003210
0	0	0	0	0	0	0	0	00003220
0	0	0	0	0	0	0	0	00003230
0	0	0	0	0	0	0	0	00003240
0	0	0	1	1	1	0	1	00003250
0	0	0	0	0	0	1	0	00003260
0	0	0	0	0	1	0	0	00003270
0	0	0	0	1	1	0	0	00003280
0	0	0	0	0	0	0	0	00003290
0	0	0	0	0	0	0	0	00003300

0	0	0	0	0	0	1	2	00003310
0	0	1	1	2	1	1	0	00003320
1	1	0	0	0	0	0	1	00003330
0	0	0	0	0	1	1	1	00003340
0	0	0	0	1	1	0	1	00003350
0	0	0	1	0	0	0	1	00003360
0	0	0	0	0	0	0	2	00003370
0	0	0	0	2	2	2	2	00003380
2	2	2	2	2	0	0	0	00003390
1	0	0	0	0	0	0	0	00003400
1	0	0	0	0	0	0	0	00003410
0	0	0	0	0	0	0	0	00003420
0	0	0	0	0	0	0	0	00003430
0	0	0	0	0	0	0	0	00003440
2	0	0	0	0	0	0	0	00003450
0	0	0	0	0	0	0	0	00003460
0	0	0	0	0	0	0	0	00003470
0	0	0	0	0	0	0	0	00003480
0	0	0	0	0	0	0	0	00003490
0	0	0	0	0	0	2	0	00003500
0	0	0	2	2	2	2	2	00003510
0	0	0	2	0	0	0	0	00003520
0	0	1	1	2	1	2	2	00003530
2	2	2	2	2	0	2	2	00003540
0	1	1	1	0	2	2	0	00003550
0	0	0	1	0	2	2	2	00003560
0	0	1	1	2	2	0	2	00003570
0	0	2	2	2	1	2	2	00003580
2	2	2	2	2	1	1	2	00003590
0	2	0	2	1	1	1	0	00003600
0	0	0	0	0	0	0	2	00003610
0	0	0	0	1	2	2	2	00003620
1	0	0	0	0	2	2	1	00003630
0	0	0	0	1	2	2	0	00003640
0	1	0	0	2	0	2	2	00003650
0	0	0	2	2	1	2	0	00003660
0	0	1	1	2	1	0	0	00003670
0	0	0	0	2	0	0	0	00003680
2	2	1	1	0	0	2	2	00003690
2	2	2	0	0	0	2	0	00003700
2	2	2	2	0	0	2	0	00003710
2	2	0	0	0	0	2	0	00003720
2	0	0	0	0	0	2	0	00003730
2	0	0	0	0	0	2	0	00003740
2	0	0	0	0	2	2	1	00003750
0	0	0	2	2	2	2	0	00003760
0	0	0	2	0	0	0	0	00003770
0	0	0	1	0	0	0	2	00003780
0	0	0	0	0	0	2	0	00003790
0	0	0	0	0	0	2	2	00003800
1	0	0	0	1	0	0	2	00003810
0	0	0	0	0	1	0	2	00003820
1	1	1	1	0	0	0	2	00003830
0	0	0	0	0	0	2	0	00003840
0	2	2	0	0	0	0	0	00003850

2	2	0	0	0	0	0	0	00003860
0	0	0	0	0	0	0	0	00003870
0	0	0	0	0	0	0	0	00003880
0	0	0	0	3	3	0	3	00003890
3	3	3	3	3	3	0	3	00003900
2	3	3	3	3	3	3	0	00003910
2	3	0	3	3	3	3	3	00003920
3	3	0	0	0	2	3	3	00003930
3	3	3	0	3	3	0	3	00003940
3	3	3	0	3	3	0	3	00003950
0	3	3	0	3	3	3	3	00003960
0	0	3	3	3	3	3	3	00003970
0	0	3	0	3	3	0	0	00003980
0	0	3	0	3	3	3	0	00003990
0	0	0	0	3	3	3	0	00004000
0	0	0	0	1	0	0	0	00004010
0	0	0	0	1	0	0	0	00004020
0	0	0	0	1	0	0	0	00004030
0	0	0	0	1	0	0	0	00004040
0	0	0	0	0	0	0	0	00004050
0	0	0	0	0	0	0	0	00004060
0	0	0	0	0	0	0	0	00004070
0	0	0	0	0	0	0	0	00004080
0	0	0	1	0	0	0	0	00004090
0	1	1	0	0	0	0	0	00004100
1	0	0	0	1	0	0	0	00004110
0	0	0	0	0	0	0	0	00004120
0	0	0	0	0	0	1	2	00004130
0	0	0	0	0	0	0	1	00004140
0	0	0	0	0	0	0	1	00004150
0	0	0	0	0	0	0	1	00004160
0	0	0	0	0	0	0	0	00004170
0	0	0	0	0	0	0	0	00004180
0	0	0	2	2	0	0	1	00004190
0	2	2	2	2	2	0	2	00004200
2	2	2	0	1	2	2	2	00004210
1	0	0	0	0	2	0	0	00004220
0	0	0	0	2	1	0	0	00004230
0	0	0	0	2	0	0	0	00004240
0	0	2	2	1	1	1	1	00004250
2	2	2	0	0	1	0	0	00004260
1	2	2	0	0	0	0	0	00004270
2	2	2	0	0	1	2	2	00004280
0	0	2	0	1	2	2	0	00004290
0	2	2	1	1	2	0	0	00004300
0	2	0	0	0	0	0	0	00004310
2	2	0	0	0	0	0	0	00004320
3	3	3	3	3	3	3	3	00004330
3	3	3	3	3	3	3	3	00004340
3	3	3	3	3	3	3	3	00004350
3	3	3	3	3	3	3	3	00004360
3	3	3	3	3	3	3	3	00004370
3	3	3	3	3	3	3	3	00004380
3	3	3	3	3	3	3	3	00004390
3	3	3	3	3	3	3	3	00004400

3	3	3	3	3	3	3	3	00004410
3	3	3	3	3	3	3	3	00004420
3	3	3	3	3	3	3	3	00004430
3	3	3	3	3	3	3	3	00004440
3	3	3	3	3	3	3	3	00004450
3	3	3	3	3	3	3	3	00004460
3	3	3	3	3	3	3	3	00004470
3	3	3	3	3	3	3	3	00004480
3	3	3	3	3	3	3	3	00004490
3	3	3	3	3	3	3	3	00004500
3	3	3	3	3	3	3	3	00004510
3	3	3	3	3	3	3	3	00004520
3	3	3	3	3	3	3	3	00004530
3	3	3	3	3	3	3	3	00004540
3	3	3	3	3	3	3	3	00004550
3	3	3	3	3	3	3	3	00004560
2	0	0	0	0	0	2	2	00004570
2	2	2	0	0	0	2	0	00004580
0	0	2	0	0	0	2	0	00004590
0	0	1	0	0	2	2	0	00004600
0	1	0	0	0	2	0	0	00004610
0	1	0	0	0	2	2	0	00004620
0	0	0	0	0	0	2	2	00004630
0	0	0	0	0	0	2	2	00004640
3	3	3	3	3	3	3	3	00004650
3	3	3	3	3	3	3	3	00004660
3	3	3	3	3	3	3	3	00004670
3	3	3	3	3	3	3	3	00004680
3	3	3	3	3	3	3	3	00004690
3	3	3	3	3	3	3	3	00004700
3	3	3	3	3	3	3	3	00004710
3	3	3	3	3	3	3	3	00004720
3	3	3	3	3	3	3	3	00004730
3	3	3	3	3	3	3	3	00004740
3	3	3	3	3	3	3	3	00004750
3	3	3	3	3	3	3	3	00004760
3	3	3	3	3	3	3	3	00004770
3	3	3	3	3	3	3	3	00004780
3	3	3	3	3	3	3	3	00004790
3	3	3	3	3	3	3	3	00004800

0	0	0	0	0	0	0	0	0000001
0	0	0	0	0	0	0	0	0000002
0	0	0	0	0	0	0	0	0000003
0	0	0	0	0	0	0	0	0000004
0	0	0	0	0	0	0	0	0000005
0	0	0	0	0	0	0	0	0000006
0	0	0	0	0	0	0	0	0000007
0	0	0	0	0	0	0	0	0000008
0	0	0	0	0	0	0	0	0000009
0	0	0	0	0	0	0	0	000001A
0	0	0	0	0	0	0	0	0000011
0	0	0	0	0	0	0	0	0000012
0	0	0	0	0	0	0	0	0000013
0	0	0	0	7	7	7	7	0000014
0	0	0	0	1	1	1	1	0000015
0	0	0	0	1	1	1	1	0000016
0	0	0	0	10	10	10	10	0000017
0	0	0	0	8	8	8	8	0000018
0	0	0	0	8	8	8	8	0000019
0	0	0	0	8	8	8	8	000002A
0	0	0	0	8	8	8	8	0000021
0	0	0	0	8	8	8	8	0000022
0	0	0	0	2	2	8	8	0000023
0	0	0	0	2	2	2	2	0000024
1	1	1	1	1	1	0	0	0000025
1	1	1	1	1	1	1	0	0000026
1	1	1	1	1	1	1	0	0000027
1	1	1	1	1	1	1	1	0000028
1	1	1	1	1	1	1	1	0000029
1	1	1	1	1	1	1	1	0000030
0	7	1	1	1	1	1	1	0000031
0	7	7	7	7	7	7	7	0000032
1	1	1	1	1	7	7	7	0000033
1	1	1	1	7	4	4	4	0000034
7	7	7	7	7	7	7	1	0000035
7	7	7	7	7	1	1	7	0000036
7	7	1	1	1	1	1	9	0000037
7	1	1	1	1	1	7	8	0000038
1	1	1	1	1	7	9	2	0000039
1	1	10	10	9	8	2	2	0000040
10	2	2	8	8	2	2	2	0000041
8	8	8	8	2	2	2	2	0000042
8	2	2	2	2	2	2	2	0000043
2	2	2	2	2	8	8	8	0000044
2	2	2	2	2	8	11	11	0000045
2	8	8	2	8	8	11	11	0000046
8	8	8	8	8	8	2	2	0000047
2	2	8	2	8	2	2	2	0000048
0	0	0	2	2	2	11	2	0000049
0	0	2	2	2	2	2	11	0000050
2	2	2	2	2	2	2	11	0000051
10	2	2	2	2	2	2	2	0000052
1	18	16	16	16	16	16	16	0000053
1	18	13	13	15	15	16	16	0000054
1	1	14	17	16	16	16	3	0000055

```
 7   7   1  10   2   2   2   2                    00000560
 7   7   9   2   2   2   2   2                    00000570
 7   4   4   7   2   2   2   2                    00000580
 8   8   8   8   2   8   8   8                    00000590
 8   8   8   8   8   8   8   8                    00000600
 2   8   2   8   8   8   8   8                    00000610
 8   8   2   8   8   8   8   8                    00000620
 8   2   8   8   8   2   8   8                    00000630
 8   8   8   8   8   8   8  11                    00000640
 2   2   2   8   2   2  11  12                    00000650
 2   2   8   8   2   2  12   8                    00000660
 8   8   8   8  11  11   8  11                    00000670
 8   8  11  11  11  11   8  11                    00000680
 2   2  11  11  11   8   8  11                    00000690
11  11  11  11  12  12   2  11                    00000700
11  11  11   2  11  11   2  11                    00000710
 2  11  11  11   2   2   2   2                    00000720
 2   8   2   2  11   0   0   0                    00000730
11   8   2   2  11  11  11  11                    00000740
12  12  11  11   2   2   2   2                    00000750
12  11  11   2   2   2   2   2                    00000760
 8   2   2   2   2   2   2   2                    00000770
 8   2   2   2   2   2   2   2                    00000780
15  16   2   2   2   2   2   2                    00000790
16  16   2   2   2   2   2   2                    00000800
 2  16  16   2   2   2   2   2                    00000810
 2   2   2   2  11   2   2   8                    00000820
 8   8   8  12  12   4   4   4                    00000830
 8   4   8   8   8   4   4   8                    00000840
 8   8   8   8   8   8   8  11                    00000850
 8   8  12  12   8   8  12  11                    00000860
11  11  12  12  12  12  11  11                    00000870
12   8  12  11  11   2   2   2                    00000880
 8  12  11  11  11   2   2   2                    00000890
11  11  11  11  11   2   2   2                    00000900
11  11  11   2  11   2   2   2                    00000910
11   2   2   2  11  11   2   2                    00000920
11  11   2   2   2  11  11   2                    00000930
11  11   2   2   2   2   2   2                    00000940
11   2   2   2   2   2   2   2                    00000950
 2   2   2   2   2   2   2   2                    00000960
11  11   2  11   2   2   2   2                    00000970
 2   2   2   2   2   2   2   2                    00000980
 2   2   2  11   2   2   2   2                    00000990
 2   2  11  11  11   2   2   2                    00001000
 2   2  11   2   2   2   2   2                    00001010
 2   2  11   2   2  11   2   2                    00001020
 2   2   2   2   2  11  11  11                    00001030
 8   8   2   8   8  11  11  11                    00001040
 8   8   8   8   8   8   8  12                    00001050
 4   4   4   8   2   2  12   8                    00001060
 4   4   8   2   2   2   2   2                    00001070
 8   8   8   2   2   2   2   2                    00001080
 2   2   2   2   2   2   2   2                    00001090
11  11  11   2   2   2   2   2                    00001100
```

11	2	2	2	2	2	2	2	0000111
2	2	2	2	2	2	2	2	0000112
2	2	2	2	2	2	2	2	0000113
2	2	2	2	2	2	2	2	0000114
2	2	2	2	2	2	2	2	0000115
11	11	11	11	2	2	2	2	0000116
11	11	11	11	11	11	11	2	0000117
2	2	19	20	20	11	2	2	0000118
2	11	11	19	19	19	19	2	0000119
2	11	2	2	19	19	19	2	0000120

APPENDIX B

PLOTS OF INCIDENCE ANGLE VARIATIONS FOR BEAM 1, 2, 3